Derivation of pluripotent stem cells from nascent undifferentiated teratoma

著者	Yuri An, Tamotsu Sekinaka, Yukiko Tando, Daiji Okamura, Keiko Tanaka, Ito-Matsuoka Yumi, Asuka Takehara, Nobuo Yaegashi, Yasuhisa Matsui
journal or publication title	Developmental Biology
volume	446
number	1
page range	43-55
year	2018-12-06
URL	http://hdl.handle.net/10097/00128033

doi: 10.1016/j.ydbio.2018.11.020

Derivation of pluripotent stem cells from nascent undifferentiated teratoma

Yuri An[1,2], Tamotsu Sekinaka[1], Yukiko Tando[1], Daiji Okamura[3], Keiko Tanaka[1,4], Yumi Ito-Matsuoka[1] Asuka Takehara[1], Nobuo Yaegashi[4] and Yasuhisa Matsui[1,2,5,6*]

[1]Cell Resource Center for Biomedical Research, Institute of Development, Aging and Cancer (IDAC), Tohoku University, Sendai, Miyagi, Japan

[2]Graduate School of Life Sciences, Tohoku University, Sendai, Miyagi, Japan

[3]Department of Advanced Bioscience, Graduate School of Agriculture, Kindai University, Nakamachi, Nara, Japan

[4]Department of Obstetrics and Gynecology, Tohoku University Graduate School of Medicine, Sendai, Miyagi, Japan

[5]The Japan Agency for Medical Research and Development-Core Research for Evolutional Science and Technology (AMED-CREST), Chuo-ku, Tokyo, Japan

[6]Center for Regulatory Epigenome and Diseases, Tohoku University School of Medicine, Sendai, Miyagi, Japan

[*]Corresponding author: yasuhisa.matsui.d3@tohoku.ac.jp (YM)

Abstract

Teratomas are tumors consisting of components of the three germ layers that differentiate from pluripotent stem cells derived from germ cells. In the normal mouse testis, teratomas rarely form, but a deficiency in *Dead-end1* (*Dnd1*) in mice with a 129/Sv genetic background greatly enhances teratoma formation. Thus, DND1 is crucial for suppression of teratoma development from germ cells. In the *Dnd1* mutant testis, nascent teratoma cells emerge at E15.5. To understand the nature of early teratoma cells, we established cell lines in the presence of serum and leukemia inhibitory factor (LIF) from teratoma-forming cells in neonatal *Dnd1* mutant testis. These cells, which we designated cultured *Dnd1* mutant germ cells (CDGCs), were morphologically similar to embryonic stem cells (ESCs) and could be maintained in the naïve pluripotent condition. In addition, the cells expressed pluripotency genes including *Oct4*, *Nanog*, and *Sox2*; differentiated into cells of the three germ layers in culture; and contributed to chimeric mice. The expression levels of pluripotency genes and global transcriptomes in CDGCs as well as these cells' adaption to culture conditions for primed pluripotency suggested that their pluripotent status is intermediate between naïve and primed pluripotency. In addition, the teratoma-forming cells in the neonatal testis from which CDGCs were derived also showed gene expression profiles intermediate between naïve and primed pluripotency. The results suggested that germ cells in embryonic testes of *Dnd1* mutants acquire the intermediate pluripotent status during the course of conversion into teratoma cells.

Key Words

germ cell, teratoma, pluripotent stem cell, Dnd1, mouse

1. Introduction

Primordial germ cells (PGCs) are undifferentiated germ cells in embryos, and normally develop into eggs or sperm. In culture, PGCs can be reprogrammed to pluripotent stem cells (PSCs), also called embryonic germ cells (EGCs), by specific cytokines (Matsui et al., 1992; Resnick et al., 1992) and/or small molecule compounds (Leitch et al., 2013). Spermatogonial stem cells (SSCs) also develop into PSCs in the presence of certain cytokines (Kanatsu-Shinonara et al., 2004). All these PSCs can contribute to chimeric

mice, indicating that their primitive pluripotency is similar to that of the pre-implantation epiblast and embryonic stem cells (ESCs) that are derived from the epiblast; this state is referred to as naïve pluripotency. Cell lines derived from the post-implantation epiblast, which are called epiblast stem cells (EpiSCs), possess more restricted pluripotency, which is referred to as primed pluripotency (Nichols and Smith, 2009).

In some conditions, teratomas, which are believed to arise from undifferentiated germ cells, develop in vivo and consist of differentiated tissues and cells of the three germ layers (Stevens and Little, 1954). Teratomas are rarely found in mice, but specific genetic backgrounds such as the 129/Sv strain and/or mutations including *Ter* markedly enhance teratoma development (Stevens, 1973; Noguchi and Noguchi, 1985). In humans, about one-third of childhood testicular cancers are teratomas (Bustamante-Marin et al., 2013). In teratocarcinomas, pluripotent embryonic carcinoma cells (ECCs) are retained. A number of ECC lines have been established from teratocarcinomas in mice and humans, and studies have reported that ECC lines are pluripotent (Kleinsmith and Pierce Jr., 1964; Mintz and Illmensee, 1975; Papaioannou et al., 1978). However, their pluripotency is sometimes restricted (Kelly and Gatie, 2017) compared to that of ESCs and EGCs.

Dnd1 was identified as a gene that is allelic with the *Ter* mutation (*Dnd1*$^{ter/ter}$) (Youngren et al., 2005). In *Dnd1*$^{ter/ter}$ mice, a point mutation that introduces a stop codon is present in the third exon of *Dnd1*. *Dnd1* encodes an RNA-binding protein that has been shown to associate with uridine-rich regions in the 3′-untranslated region of target mRNAs, thereby protecting the mRNAs from microRNA-mediated translation repression (Kedde et al., 2007). A recent study reported that DND1 destabilizes target mRNAs via recruitment of the CCR-NOT deadenylase complex in PGCs and SSCs (Yamaji et al., 2017). These results suggest that DND1 either stabilizes or destabilizes different target mRNAs via distinct mechanisms in germ cells. Previous studies identified *Cdkn1a* and *Cdkn1b*, which encode negative regulators of the cell cycle (p21^{cip1} and p27^{Kip}, respectively) and whose expression is down-regulated in germ cells in *Dnd1*$^{ter/ter}$ embryos, as teratoma-related target mRNAs of DND1 (Cook et al., 2011). We also found that DND1 targets the transcript encoding Ezh2, a histone H3K27 trimethyl transferase, which causes down-regulation of the cell cycle control protein CCND1, in germ cells (Gu et al., 2018). These results together suggest that enhancement of the cell cycle is likely a key event in the conversion of germ cells into teratomas. Although pluripotent ECC lines can be obtained from well-developed teratocarcinomas, the nature of the ECC lines derived

from nascent teratoma cells has not been reported.

In *Dnd1*$^{ter/ter}$ embryonic testes, only a few germ cells are found, but some of these germ cells start to proliferate and form small clusters of nascent teratoma cells at embryonic day 15 (E15) (Stevens, 1971). In our previous study, we detected cell clusters expressing pluripotency markers such as 4C9 and SSEA1 by E17.5 (Gu et al., 2018). We designated these cells, which likely initiate teratoma development, as teratoma-forming cells. Although the emergence of differentiated cells in nascent teratomas in perinatal testes suggests that the teratoma-forming cells are pluripotent, the detailed cellular status of the teratoma-forming cells has not been described and is important for further understanding the process of conversion of germ cells into teratoma-forming cells. In this study, we show the derivation and characterization of cell lines from teratoma-forming cells in *Dnd1*$^{ter/ter}$ testes. Our results suggest that cell lines derived from early teratoma cells show an intermediate cellular status between naïve and primed pluripotency.

2. Materials and methods

2.1 Mice and genotyping

Oct4-deltaPE-GFP transgenic mice with the B6D2F1 background (Yoshimizu et al., 1999) were backcrossed to 129/Sv/*Dnd1*$^{ter/+}$ mice obtained from The Jackson Laboratory for more than 10 generations to establish a congenic strain of 129Sv/*Dnd1*$^{ter/+}$/Oct4-deltaPE-GFP mice. Female and male 129Sv/*Dnd1*$^{ter/+}$/Oct4-deltaPE-GFP mice were mated in the afternoon, and the presence of vaginal plugs was checked the next morning. The day on which a plug was found was considered to be E0.5. DNA was extracted from the tail of the embryos, and was genotyped using the primer set TerF:5'-TCCAGGAGACACTGCTGCTA-3' and TerR:5'- TTCAGGAACTCCACTTGTGC-3' according to the protocol provided on The Jackson Laboratory website (https://www2.jax.org/protocolsdb/f?p=116:5:0::NO:5:P5_MASTER_PROTOCOL_ID,P5_JRS_CODE:2172,000091). The mice were kept and bred in the Animal Unit of the Institute of Development, Aging and Cancer, Tohoku University, which is a controlled-environment and pathogen-free facility, according to the guidelines for the care and use of experimental animals defined by the facility. Animal protocols were reviewed and approved by the Tohoku University Animal Studies Committee.

2.2 HE staining and Immunohistochemistry

Embryonic gonads were collected from embryos on E18.5 to P7 in DMEM containing 10% fetal bovine serum (FBS). Gonads were fixed in Bouin for overnight at 4°C. Samples were embedded in paraffin after dehydrtation, and were sectioned at 4 μm, which were further processed for HE staining or immunostaining. For frozen sections, Gonads were fixed in 4% paraformaldehyde (PFA) for 3h at 4°C. Fixed gonads were then soaked in 10% sucrose for 1 h at 4°C, and then in 20% sucrose overnight at 4°C. Samples were embedded in O.C.T. compound (Tissue Tek), and were sectioned at 8 μm. For immunostaining, the sections were blocked in 5% skim milk/1% Triton X-100 in phosphate-buffered saline (PBS), and were incubated overnight at 4°C in the primary antibodies diluted in 1% skim milk/0.1% Triton X-100 in PBS. For cultured cells, samples were fixed in 4% PFA for 3h at room temperature, and treated in 1% Triton X-100 in PBS for 15 min, then blocked in 10% FBS/1% BSA/0.1% Triton X-100 in PBS for 1h. Samples were incubated for overnight at 4°C in the primary antibodies diluted in the same solution as for blocking; the antibodies included rat anti-4C9 (1:150 dilution; Yoshinaga et al., 1991), rat anti-SSEA1 (1:100 dilution; Santa Crus, sc-21702), mouse anti-α smooth muscle actin (1:600 dilution; Sigma-Aldrich, A5228), rabbit anti-β tubulin (1:1000 dilution; Sigma-Aldrich T2200), mouse anti-Foxa2 (HNF3β) (1:100 dilution; Santa Cruz, sc-374376), goat anti-Otx2 (1:200 dilution; R&D; AF1979), mouse anti Oct4 (1:300 dilution; Santa Cruz; sc-5279). After washing, sections or cells were incubated with HRP anti-rat IgG (1:200 dilution), HRP anti-mouse IgG (1:200 dilution), Alexa Fluor 568 anti-rabbit IgG (1:500 dilution; Invitrogen), Alexa Fluor 568 anti-rat IgG (1:500 dilution; Invitrogen), Alexa Fluor 568 anti-mouse IgG (1:500 dilution; Invitrogen) or AlexsaFlior 568 anti-goat IgG (1:500 dilution; Invitrogen) for 1 h at room temperature. For fluorescence, samples were stained with 1μg/ml DAPI or Hoechst33342. Images were taken using a Leica AF6000 Microscope or SP8 Confocal Microscope.

2.3 Derivation and culture of CDGCs

All cells were cultured in an atmosphere of 5% CO_2 at 37°C. Oct4-deltaPE-GFP expressing cell clusters were manually isolated from *Dnd1*$^{ter/ter}$ testis at P2 and dissociated them by 1x Trypsine/EDTA (Sigma), then seeded on Mitomycin C-treated feeder layer of mouse embryonic fibroblast (MEF) in 96-well plate (Falcon) with medium containing G-MEM (Gibco), 10% FBS, 10 μM MEM Non-Essential Amino Acids (Gibco), 1 mM

sodium pyruvate (Gibco), 100 μM 2-mercaptoethanol, and 1000 U/μl leukemia inhibitory factor (LIF) (Millipore). For subculture, the cells were dissociated by 1x Trypsin/EDTA and seeded on a fresh feeder layer. After two to five times subculture, single colonies were isolated and seeded on a fresh MEF feeder layer after dissociation to establish CDGC lines. The cell lines were maintained in the same medium or in N2B27 (Gibco) supplemented with 1000U/μl LIF, 1 μM PD0325901 and 3 μM CHIR99021(2i). The cell lines were also cultured in EpiSC medium (N2B27 medium containing activin A (20 ng/ml; Peprotech), bFGF (12 ng/ml; Invitrogen), and KSR (20%; Invitrogen)), and were passaged every 3 days by dissociating with collagenase IV (1 mg/ml; Invitrogen) on MEF feeder (Hayashi et al., 2011).

2.4 Induction of CDGC differentiation

CDGCs were induced to cardiac muscle cells as described previously (Hescheler et al., 1997). CDGCs labeled with Oct4-deltaPE-GFP were purified by cell-sorting (S3e Cell Sorter, Bio-Rad), and were suspended in medium containing alpha-MEM (Gibco), 10% FBS, 10 μM MEM Non-Essential Amino Acids (Gibco), 1 mM sodium pyruvate (Gibco), 2 mM L-glutamine (Gibco), 100 μM 2-mercaptoethanol at 2.5×10^4 cells/ml. 20 μl of the cell suspension was culture in hanging drops for four days to form embryoid bodies. Two or three embryoid bodies were transferred to a well of gelatin-coated 24-well plate in the same medium and were cultured until beating cells were found. Differentiation to neural cells was carried out as described with minor modifications (Watanabe et al., 2005). 20 μl of cell suspension of CDGCs in medium containing G-MEM (Gibco), 5% KSR (Gibco), 10 μM MEM Non-Essential Amino Acids (Gibco), 1 mM sodium pyruvate (Gibco), 100 μM 2-mercaptoethanol at 5.6×10^4 cells/ml was cultured in hanging drops for 5 days. The embryoid bodies were transferred to gelatin-coated 24-well plates in the same medium with 100-200 embryoid bodies/cm^2 and were cultured for three days. For differentiation to endodermal cells (Ueda et al., 2010), 15 μl of cell suspension of CDGCs in medium containing D-MEM (Gibco), 10% FBS, 10 μM MEM Non-Essential Amino Acids (Gibco), 1 mM sodium pyruvate (Gibco), 100 μM 2-mercaptoethanol, 1x penicillin/streptomycin at 3.3×10^4 cells/ml was cultured in hanging drops for 6 days. 50 embryoid bodies were transferred to a well of 6-well plates in the same medium and were cultured for 21 days.

2.5 Production of chimeric mice

Production of chimeric mice was carried out as described (Matsui et al., 2014). Approximately 10 CDGC1-P3-9 cells cultured in 2i/LIF condition were injected into each blastocyst obtained from MCH mice (Japan SCL), and then transferred into the uterus of pseudo-pregnant female MCH mice.

2.6 ESC culture and Dnd1 knock-down

For *Dnd1* knock-down (KD), shRNA vector (pKLO.1-shDnd1, Gu et al., 2018) or control empty vector (pKLO.1) was transfected to E14tg2a ESCs by using Lipofectamine 2000 (Invitrogen) according to the manufacturer's instruction. The E14tg2a ESCs were cultured in the same serum/LIF medium for culturing CDGCs without feeder cells. 2μg/ml of Puromycin was added after 6 h for selecting cells harboring the introduced gene, and the cells were recovered after 36 h to purify total RNA. We confirmed that the expression of *Dnd1* was decreased to about 15% of the expression in control cells (data not shown). BVSC ESCs (Hayashi et al., 2011; kindly gifted by Dr. M. Saitou) were culture in 2i/LIF medium without feeder cells, and induced to EpiLCs as described (Hayashi et al., 2011). D3 ESCs were cultured in the serum/LIF medium on MEF feeder.

2.7 Mouse EpiSCs Culture

Mouse EpiSCs (kindly gifted by Dr. H. Niwa) were cultured on gelatin-coated dishes with MEF (mouse embryonic fibroblasts) in DMEM/F-12 (Gibco) supplemented with 20% KSR (Gobco), 0.1 mM non-essential amino acid (NEAA; Gibco), 1 mM sodium pyruvate (Gibco), 0.2 mM L-glutamine (Sigma), 0.1 mM β-mercaptoethanol (Sigma), 10 ng/ml Activin A (R&D), and 5 ng/ml bFGF (Sigma).

2.8 RT-qPCR

Total RNA was purified from FACS-purified GFP-positive CDGCs, *Dnd1*-KD or control ESCs by RNeasy Plus Mini Kit (QIAGEN) by RNeasy Micro Kit (QIAGEN) according to the manufacturer's instruction. Using random primers and SuperScript III Reverse Transcriptase (Invitrogen), cDNA was synthesized. 2× Power SYBR Green PCR Master Mix (Applied Biosystems) was used for real-time qPCR in 20 μl of reaction solution containing 1 μl of cDNA, 8 μl of Milli-Q water, and 1 μl of 10 μM gene-specific forward and reverse primers. Arbp was used as an internal control. The primer sequences are

shown in Table S3. qPCR was performed using a CFX Connect Real-Time System (Bio-Rad). The cycling conditions were as follows: 50°C for 2 min (one cycle); 95°C for 10 min (one cycle); and 95°C for 15 s and 60°C for 2 min (45 cycles).

2.9 RNA-seq

CDGCs labeled with Oct4-deltaPE-GFP were cultured in serum/LIF medium on MEF feeder, Dnd1-KD E14tg2a ESC and control E14tg2a ESCs (129/Ola background) were purified by cell-sorting (S3e Cell Sorter, Bio-Rad). RNA-seq libraries were prepared from 500 ng of total RNA purified from CDGC1-P3-9, CDGC6-P5-6, *Dnd1*-KD ESCs and control ESCs of two biological replicates, with TruSeq RNA sample prep kit v2 (Illumina). The libraries were clonally amplified on a flow cell and sequenced on HiSeq2500 (HiSeq Control Software v2.2.58, Illumina) with 51-mer single-end sequence. Image analysis and base calling were performed using Real-Time Analysis Software (v1.18.64, Illumina). For gene expression analysis, reads were mapped to the mouse genome (UCSC mm10 genome assembly and NCBI RefSeq database) using TopHat2 and Bowtie. Cufflinks was used to estimate gene expression levels based on reads per kilobase of exon per million mapped reads (RPKM) normalization. Differentially expressed genes (DEGs) were extracted from the Cuffdiff results with statistical significance ($q<0.05$). DAVID Bioinformatics Resources 6.8 was used for pathway analysis, and GeneSpring (Tomy Degital Bio) was used for generating scatter plots and PCA. The GEO accession number for the RNA-seq data reported in this manuscript is GSE118582. RNA-seq data (two biological replicates in each sample except for EpiSC_1 and E16.5_mGC) were also obtained from data base; D3 GFP ESC (129Sv background; SRR827706, SRR827707; Brady et al., 2013), EpiSC_1 (129Sv background; SRR3317447; Fiorenzano et al., 2016), EpiSC_2 (B6 background; SRR1660269, SRR1660270; Wu et al., 2015), E11.5 male(m)PGCs (B6 background; SRR648693, RSS648694; Yamaguchi et al., 2012), E13.5 mPGCs (B6 background; SRR649339, SRR649340; Yamaguchi et al., 2012), and E16.5 male germ cells (mGC) (B6 background; ERR192339; Seisenberger et al., 2012)

2.10 Bisulfite sequencing of imprinted genes

Bisulfite sequencing was carried out as described (Sekinaka et al., 2016). Genomic DNA was extracted from sorted Oct4-deltaPE-GFP positive CDGCs cultured in serum/LIF

medium using DNeasy Blood & Tissue kits (QIAGEN). 10 ng of genomic DNA was converted with sodium bisulfite using the EZ DNA Methylation-Direct Kit (Zymo Research) according to manufacturer's instructions. The targeted regions of *H19, Igf2* and *Snrpn* were amplified by nested PCR from bisulfite-converted DNAs using BIOTAQ HS DNA Polymerase (BIOLINE). The sequences of the PCR primers used for this assay are listed in Table S3 (Kim et al., 2013). The PCR products were purified 1.5% agarose gel electrophoresis and the QIAquick Gel Extraction Kit (QIAGEN). The purified-samples were cloned into pGEM-T easy vectors (Promega) and were sequenced using SP6 primer and the BigDye Terminator v1.1 Cycle Sequencing Kit (Applied Biosystems). The sequence data were analyzed with the QUantification tool for Methylation Analysis (http://quma.cdb.riken.jp/top/index.html).

2.11 Single cell RT-qPCR

Oct4-deltaPE-GFP expressing single cells from *Dnd1*$^{ter/ter}$ testis at P2, and BVSC ESCs cultured in 2i/LIF medium were manually isolated after trypsin treatment. Preparation of cDNA form single cells was carried out as described previously with minor modifications (Kurimoto et al., 2006). A single cell with 0.5 µl of PBS was put in 4.5 µl of Lysis Mix (10 mM Tris-HCl, 50 mM KCl, 1.5 mM $MgCl_2$, 0.5% NP-40, 5 mM DTT (Invitrogen), 0.2 ng/µl Primer V1, 0.4 units/µl RNase inhibitor (Promega), 0.2 mM dNTPs (Roche)). Primer sequences are shown in Table S3. After centrifugation at 6,700 x g for 15 sec, cell lysates were incubated at 70 °C for 90 sec and 4 °C for 1 min. 40 units (0.2 µl) of SuperScript III, 1 units (0.025 µl) of RNase inhibitor and 0.875 µl of MillQ water were added to each sample which was further incubated at 50 °C for 60 min, 70 °C for 10 min and 4 °C for 1 min. After centrifugation at 16,100 x g for 10 sec, 0.1 µl of Endonuclease buffer (New England Biolabs) and 0.5 units (0.025µl) of Endonuclease I (New England Biolabs) were added to each sample which was further incubated at 37 °C for 30 min, 80 °C for 25 min and 4 °C for 1 min. After centrifugation at 16,100 x g for 10 sec, 6 µl of TdT Mix (10 mM Tris-HCl, 50 mM KCl, 1.5 mM $MgCl_2$, 3 mM dATP (Roche), 0.1 units/µl of RNase H (Invitrogen), 0.8 units/µl of TdT (Roche)) was added to each sample which was incubated at 37 °C for 15 min, 70 °C for 10 min and 4 °C for 1 min. 3 µl aliquots of each sample were added to 19 µl of PCR Mix I (1x ExTaq Buffer (Takara), 1 mM dNTPs, 0.05 units/µl ExTaq polymarase (Takara), 0.02 µg/µl Primer V3). After centrifugation at 2,000 x g for 10 sec, samples were incubated at 95 °C for 3 min, 50 °C

for 2 min, 72 °C for 3 min and 4 °C for 1 min. After centrifugation at 2,000 x g for 10 sec, 19 µl of PCR Mix II (1x ExTaq Buffer, 1 mM dNTPs, 0.05 units/µl ExTaq polymarase, 0.02 µg/µl Primer V1) was added to each sample, and centrifugation at 2,000 x g for 10 sec. Samples were then incubated at 95 °C for 30 sec, 67 °C for 1 min, 72 °C for 3 min (+ 6 sec in each cycle) (20 cycles) and were kept at 4 °C. Samples were then purified by QIA quick column (QIAGEN) with 50 µl of final elution volume. 1 µl of each sample was used for RT-qPCR. The primer sequences are shown in Table S3.

2.12 Statistical analysis

Statistical analysis was performed using the Student's t-test. p-values < 0.05 were considered to be statistically significant.

3. Results

3.1 Derivation of pluripotent stem cells from the teratoma-forming cells in the Dnd1$^{ter/ter}$ testis

To identify appropriate developmental stages of the *Dnd1$^{ter/ter}$* testis for derivation of cell lines from teratoma-forming cells, we first detected SSEA1-expressing cells, which are likely pluripotent, in the *Dnd1$^{ter/ter}$* testis at different developmental stages. We found SSEA1-positive cell clusters at E18.5 (Fig. 1B), whereas Oct4-deltaPE-GFP-expressing germ cells were rarely observed in the *Dnd1$^{ter/ter}$* testis at E18 and subsequently (Gu et al., 2018). The SSEA1-positive cell clusters also were observed at post-natal days 2 and 4 (P2 and P4), but by P7, those cells had disappeared (Fig. 1B). In addition, eosin-positive areas at P4 and cavitated areas at P7, which are likely associated with differentiating teratomas, were observed (Fig. 1A). These results confirmed that SSEA1-positive cells exist in the *Dnd1$^{ter/ter}$* perinatal testis, in agreement with previous observations (Stevens, 1981), and that the testes from E18.5 to P4 may be suitable for derivation of cell lines.

To further confirm the presence of teratoma-forming cells in the P2 testis used for establishing cell lines, we assessed the expression of 4C9, an additional pluripotency marker, as well as that of the Oct4-deltaPE-GFP reporter, in the cell clusters at P2 (Fig. 2A, B) (Gu et al., 2018). We then isolated and dissociated the Oct4-deltaPE-GFP-expressing cell mass from the *Dnd1$^{ter/ter}$* testis at P2, and cultured the cells in the serum/leukemia inhibitory factor (LIF) condition, which is suitable for derivation of

mouse ESCs from pre-implantation blastocysts. One day after plating the cells, we observed isolated single Oct4-deltaPE-GFP-positive cells; by day 5 in culture, those cells had formed densely packed, dome-shaped colonies (Fig. 2C, upper two rows). We repeated the subculture 2-5 times by treating whole wells with trypsin (Fig. 2C, third row), and isolated single colonies to establish cell lines (Fig. 2C, bottom row). We designated the resulting cell lines "cultured *Dnd1* mutant germ cells" (CDGCs). We obtained seven cell lines from the first trial, one of which is CDGC1-P3-9, and six more lines from an independent primary culture, one of which is CDGC6-P5-6 (Fig. S1A). These cell lines maintained an undifferentiated cellular status after 19 cycles of subculturing. In addition, these cells were able to acquire a cultured naïve pluripotent state in 2i (PD0325901 and CHIR99021)/LIF-containing medium (Fig. 2D, Fig. S1B) (Nichols and Smith, 2009).

3.2 Gene expression profiles of CDGCs

To assess the pluripotency of CDGCs at the molecular level, we used RT-qPCR to examine the expression of pluripotency-associated genes in CDGCs cultured in the serum/LIF condition. Among pluripotency-related genes (Nichols and Smith, 2009), *Oct4*, *Nanog*, and *Sox2* exhibited higher expression in CDGCs than in primed EpiSCs, while demonstrating similar expression in CDGCs and in naïve ESCs (Fig. 3A). The expression of these core pluripotency genes in ESCs and EpiSCs was similar to each other's expression levels in several previous studies, but a low level of expression previously was reported in some EpiSCs (Murayama et al., 2015), suggesting that the expression of these genes depends on the EpiSC line.

The expression of the naïve pluripotency genes *Esrrb*, *Tbx3*, and *Klf4* was significantly lower in CDGC1-P3-9 compared with that in ESCs and similar in CDGC1-P3-9 and EpiSCs (Fig. 3B). In CDGC6-P5-6, the expression of these genes was relatively high compared with that in EpiSCs (Fig. 3B), suggesting that CDGC1-P3-9 and CDGC6-P5-6 cultured in serum/LIF medium may differ in the expression of naïve pluripotency genes.

In the case of primed pluripotency genes (Nichols and Smith, 2009), the expression of *Otx2* in CDGCs was significantly higher than that in ESCs and lower than that in EpiSCs. The expression level of *Fgf5* was nominally higher in CDGCs than in ESCs, and the expression of *Sox17* was nominally lower in CDGCs than in EpiSCs (Fig. 3C). Therefore, the expression levels of naïve and primed pluripotency genes were not consistent in CDGCs cultured in serum/LIF medium, suggesting that CDGCs have an intermediate

status between naïve and primed pluripotency with regard to the expression of pluripotency genes.

We also examined the expression of OTX2 by immunostaining. In ESCs cultured in the 2i/LIF condition and in epiblast-like cells (EpiLCs), the OTX2 signals were homogeneously weak and strong, respectively, whereas OTX2 expression was heterogeneous in CDGCs cultured in the serum/LIF condition (Fig. S2). Oct4-deltaPE-GFP-positive cells, which correspond to naïve pluripotent cells in CDGCs, showed relatively weak OTX2 expression compared to GFP-negative cells, suggesting that CDGCs in serum/LIF medium are maintained as a mixture of relatively naïve and primed pluripotent cells. After culturing in the 2i/LIF condition, CDGCs consistently showed pluripotency gene expression corresponding to naïve pluripotency (Fig. S3).

To comprehensively compare molecular signatures of CDGCs with those of ESCs, EpiSCs, and PGCs, we performed transcriptomic analysis. Specifically, we performed RNA-seq for two biological replicates each of CDGC1-P3-9, CDGC6-P5-6, E14tg2a ESCs, and Dnd1-KD E14tg2a ESC (GSE118582). We also obtained published RNA-seq data for D3 GFP ESC (SRR827706, SRR827707; Brady et al., 2013), EpiSC_1 (SRR3317447_1, SRR3317447_2; Fiorenzano et al., 2016), EpiSC_2 (SRR1660269, SRR1660270; Wu et al., 2015), E11.5 male(m)PGCs (SRR648693, RSS648694; Yamaguchi et al., 2012), E13.5 mPGCs (SRR649339, SRR649340; Yamaguchi et al., 2012), and E16.5 male germ cells (mGS) (ERR192339; Seisenberger et al., 2012).

Differentially expressed genes (DEGs) between CDGC1-P3-9 and E14tg2a ESCs, and between CDGC6-P5-6 and E14tg2a ESCs, which were cultured in the serum/LIF condition, were 13.2% and 4.1% of the total genes, respectively (Fig. 4A). DEGs between CDGC1-P3-9 and EpiSCs_1 were 14.0% of the total genes. Principal component analysis (PCA) showed that gene expression profiles of CDGC6-P5-6 were more closely related to those of ESCs, especially *Dnd1*-KD ESCs, compared to those of EpiSCs, whereas CDGC1-P3-9 was less closely related to ESCs, instead appearing to resemble EpiSCs (Fig. 4B). These results suggested that CDGC1-P3-9 and CDGC6-P5-6 possess slightly different cellular statuses, i.e., CDGC6-P5-6 is more closely related to ESCs, whereas CDGC1-P3-9 is intermediate between ESCs and EpiSCs.

To estimate the influences of *Dnd1* deficiency on ESCs, we also compared gene expression in *Dnd*1-knockdown (KD) ESCs with that in control E14 tg2a ESCs (Fig. 4A). DEGs between those cells were 2% of the total genes, indicating that deficiency in *Dnd1*

minimally affects gene expression in ESCs. Meanwhile, PCA showed that *Dnd1*-KD ESCs were closely correlated to CDGC6-P5-6, suggesting that deficiency in *Dnd1* contributes (to some extent) to transcriptomic differences between CDGCs and ESCs.

Both CDGC lines were distinct from male germ cells in embryonic gonads at E11.5 to E16.5 (Fig. 4B). Consistent with this observation, the expression levels of core and primed pluripotency genes and the male germ cell markers *Nanos2* (Suzuki and Saga, 2008) and *Dnmt3l* (Bourc'his and Bester, 2004) in CDGCs were higher and lower, respectively, than in male germ cells (Fig. S4, Table S2).

3.3 CDGCs cultured in the primed pluripotency condition

As mentioned above, CDGCs were established in the serum/LIF condition, and could be adapted to the 2i/LIF condition. Gene expression profiles suggested that CDGCs possessed an intermediate status between naïve and primed pluripotency. We further tested whether CDGCs could be adapted to a culture condition of primed pluripotency. We transferred CDGCs cultured in serum/LIF medium into EpiSC medium containing Activin A and basic fibroblast growth factor (bFGF). After three passages, many colonies were observed but these colonies became flattened, and Oct4-deltaPE-GFP expression was down-regulated, while OCT4 protein persisted in those colonies (Fig. S5). These observations suggested that CDGCs are converted to a more primed pluripotent status in the primed culture condition.

3.4 Differentiation potential of CDGCs

Gene expression profiles suggest that CDGCs are PSCs. To confirm this, we first tested differentiation of CDGCs into typical cells of the three germ layers via embryoid body formation in vitro. CDGCs gave rise to differentiated cells expressing α-smooth muscle actin (α-SMA), β-tubulin, and Forkhead box (Fox) a2, which represent mesodermal cardiac muscle, ectodermal neurons, and endodermal cells, respectively (Fig. 5A, Fig. S6). In addition, we observed that some α-SMA- and hepatocyte nuclear factor (HNF) -3β-expressing cells showed beat and peristaltic movements, respectively, consistent with expected tissue function. Therefore, CDGCs can differentiate into cells of the three germ layers.

We then introduced CDGC1-P3-9 cultured in 2i/LIF medium but not in serum/LIF medium, into blastocysts to examine their contributions to chimeric mice, because

pluripotency gene expression in CDGC1-P3-9 in the serum/LIF condition was partially distinct from a typical naïve profile (Fig. 3, Fig. S3). We found five males and five females with coat color chimerism from six pregnant females (Fig. 5B). However, the incidence of chimerism was relatively low, about 5-30%, and two mice died at 2 and 3 weeks of age, suggesting that CDGC1-P3-9 cells are not typical naïve pluripotent cells and/or have some abnormalities. The chimeric mice did not develop any tumors including teratomas. We are mating male chimeric mice with female MCH mice, but germ line transmission has not been observed so far.

3.5 Paternal imprinting is established in CDGCs

We examined whether paternal imprinting was established in CDGCs that originated from the teratoma-forming cells in P2 testes. We examined *H19* and *Igf2* as paternally imprinted genes and *Snrpn* as a maternally imprinted gene, and found that *H19* and *Igf2* were exclusively methylated, while *Snrpn* was exclusively de-methylated (Fig. 6), in both cell lines. These results suggested that paternal imprinting progresses normally in the teratoma-forming cells in neonatal testes and is maintained during the course of CDGC establishment.

3.6 Teratoma-forming cells in the Dnd1$^{ter/ter}$ testis show a pluripotency-associated gene expression profile differing from that of ESCs

To assess the similarity between teratoma-forming cells that initiate teratoma development in P2 testes and ESCs, we next compared the teratoma-forming cells in the *Dnd1$^{ter/ter}$* testis with ESCs regarding the expression of pluripotency-associated genes. We randomly picked single Oct4-deltaPE-GFP-expressing cells from the teratoma-forming cell clusters isolated from the *Dnd1$^{ter/ter}$* testis at P2, as well as single ESCs cultured in the 2i/LIF condition, and performed single-cell RT-qPCR (Kurimoto et al., 2006). Among the core and naïve pluripotency genes, *Oct4* and *Nanog* were expressed in most single cells at levels comparable to those in ESCs, whereas the expression of *Esrrb* was lower in all single cells than that in ESCs. *Sox2* and *Tbx3* showed variable expression among the single cells (Fig. 7 and Fig. S7).

Regarding the primed pluripotency genes, expression of *Fgf5* and *Otx2* was higher in the majority of single cells compared with that in ESCs, and *Sox17* showed variable expression among the single cells. Low expression of a naïve marker, *Esrrb*, and high

expression of a primed marker, *Fgf5*, in most single cells suggested that the majority of the teratoma-forming cells in P2 testis possesses a cellular status that resembles primed pluripotency. Some single cells such as #7, 8, 13, and 19 in Fig. 7 showed expression levels of *Tbx3* similar to those observed with ESCs, and expression levels of *Sox17* and *Otx2* relatively lower than those observed with the rest of the single cells, suggesting that these single cells likely possess more naïve pluripotency.

4. Discussion

We successfully derived PSC lines, which we termed CDGCs, from teratoma-forming cells in the *Dnd1*$^{ter/ter}$ testis at P2 in medium containing serum/LIF. We showed that the CDGCs can be maintained in this condition as well as in the 2i/LIF condition (Fig. 2, Fig. S1). CDGCs differentiated into cells of the three germ layers including cardiac muscle, neurons, and endodermal cells in culture and contributed to chimeric mice (Fig. 5, Fig. S6).

Pluripotency gene expression and global gene expression profiles suggested that CDGCs possess pluripotency intermediate between naïve and primed (Fig. 3, Fig. 4). In addition, CDGC1-P3-9 was easily adapted to the EpiSC culture condition (Fig. S5). Immunostaining of CDGCs with an anti-OTX2 antibody indicated that some cells in CDGCs showed higher expression of OTX2 compared to that in other cells (Fig. S2), suggesting that CDGCs are maintained as a mixture of cells with relatively naïve and primed pluripotency. The gene expression profiles suggested that CDGC6-P5-6 may be in a state resembling naïve pluripotency (Fig. 3, Fig. 4). Subtle differences in culture conditions during establishment of CDGC lines may have resulted in distinct expression of pluripotency genes in the two CDGC lines. The differential gene expression between the two CDGC lines likely reflects the nature of the teratoma-forming cells from which the CDGCs originated, because the teratoma-forming cells in the *Dnd1*$^{ter/ter}$ testis at P2 are heterogeneous with regard to the expression of some naïve and primed pluripotency genes, such as *Tbx3* and *Sox17* (Fig. 7, Fig. S7).

Single-cell RT-qPCR showed that the expression of a primed pluripotency gene, *Fgf5*, and a naïve pluripotency gene, *Esrrb*, was higher and lower, respectively, in most teratoma-forming cells than in ESCs; in contrast, other naïve and primed pluripotency genes such as *Tbx3*, *Sox17*, and *Otx2* showed variable expression levels among the

teratoma-forming cells. Together, these results suggested that pluripotency in the teratoma-forming cells in the testes is related to the primed or intermediate pluripotent status. Consistent with this hypothesis, when germ cells in embryonic testes develop teratomas, the germ cells first form an epiblast-like structure, and a recent study revealed that germ cells acquire primed pluripotency during the course of teratoma formation (Dawson et al., 2018). Previous observations indicated that immature tissues are observed at P10 (Stevens, 1981), and well-developed teratomas that appear 2-3 weeks after birth consist primarily of differentiated cells (Stevens, 1983). Our results also showed that differentiating teratoma cells were observed as early as P4 in our experimental conditions. The results together support the idea that the teratoma-forming cells are pluripotent. The teratoma-forming cells with a relatively more naïve or primed status may adapt in the serum/LIF culture condition to yield PSCs that partially reflect the original pluripotent status. Overall expression profiles of pluripotency genes in CDGCs, especially CDGC1-P3-9, resembled those of some teratoma-forming cells, suggesting that CDGCs represent, at least in part, the cellular status of the teratoma-forming cells in vivo. The efficiency of chimeric mouse formation by CDGCs was low (Fig.5B), similar to that of traditional ECCs, and some chimeric mice containing CDGCs died shortly after birth, suggesting that the pluripotency of CDGCs was not a typical naïve status.

In addition to LIF, bFGF is essential for reprogramming of PGCs into pluripotent EGCs (Mtasui et al., 1992; Resnick et al., 1992), and germ cells isolated after E14.5 rarely develop into EGCs (Kimura et al., 2007; Matsui et al., 2014). In the case of SSC-derived PSCs, glial cell-derived neurotrophic factor (GDNF) is essential, and PSCs have not been obtained from SSCs in ESC medium after several experiments (Kanatsu-Shinonara et al., 2004). In contrast, CDGCs were derived from the P2 testis in ESC medium containing LIF but not in medium containing bFGF or GDNF. This result suggested that the teratoma-forming cells are distinct from PGCs and SSCs, which are not themselves pluripotent. Consistent with this inference, transcriptomic analysis showed that gene expression in CGDCs was distinct from that in germ cells in embryonic testes (Fig. 4, Fig. S4). Nevertheless, we found that paternal imprinting was established in CDGCs (Fig. 6), suggesting that establishment of paternal imprinting proceeds normally during conversion of embryonic male germ cells into teratoma-forming cells. *Dnd1*-deficient germ cells may differentiate normally, thereby yielding gonocytes and permitting the establishment of paternal imprinting, with subsequent reprogramming to acquire

pluripotency. Alternatively, *Dnd1*-deficient germ cells may maintain potential pluripotency in PGCs while also permitting the establishment of the paternal imprinting.

Our results indicated that PSCs can be derived from the nascent teratoma-forming cells in the *Dnd1*$^{ter/ter}$ testis at P2. Because *Dnd1* deficiency did not significantly affect global gene expression in ESCs (Fig. 4), establishment of CDGCs from the teratoma-forming cells as PSCs and their adaptation to the culture condition for naïve pluripotency likely are not due to the loss of *Dnd1*. Therefore, ECCs with normal *Dnd1* also may be maintained in the naïve pluripotency condition, although this possibility will need to be tested in future studies. Additionally, more detailed analyses of teratoma-forming cells, including identification of key genes specifically expressed in the teratoma-forming cells, are expected to shed light on the molecular mechanisms of teratoma development from germ cells.

Acknowledgements

We thank Drs. K. Nakayama, R. Funayama, M. Shirota, M. Kikuchi, M. Nakagawa, and K. Kuroda for technical assistance, Dr. M. Saitou for BVSC ESCs, Dr. H. Niwa for EpiSCs, Dr. D. Okamura for antibodies, Drs. B. Capel and Y. Hayashi for critical reading of the manuscript, and all the members of Cell Resource Center for Biomedical Research for helpful discussions. We also acknowledge the technical support of the Biomedical Research Core of Tohoku University Graduate School of Medicine, and the Center of Research Instruments of Institute of Development, Aging and Cancer (IDAC), Tohoku University.

Funding

This research was supported by a Grant-in-Aid for Scientific Research (KAKENHI) in the Innovative Areas, “Mechanisms regulating gamete formation in animals” (grant #25114003) from the Ministry of Education, Culture, Sports, Science and Technology of Japan, and by AMED-CREST (grant #JP17gm0510017h) from the Japan Agency for Medical Research and Development to YM. Y.T. was supported by KAKENHI for Early-Career Scientists (grant #18K15001) and for JSPS Research Fellow (grant #18J40019).

References

Brady, J.J., Li, M., Suthram, S., Jiang, H., Wong, W.H., Blau, H.M. (2013). Early role for IL-6 signaling during generation of induced pluripotent stem cells revealed by heterokaryon RNA-Seq. Nat. Cell Biol. 15, 1244-1252.

Bourc'his, D., Bester , T.H. (2004). Meiotic catastrophe and retrotransposon reactivation in male germ cells lacking Dnmt3L. Nature 431, 96-99.

Bustamante-Marín, X., Garness, J.A., Capel, B. (2013). Testicular teratomas: an intersection of pluripotency, differentiation and cancer biology. Int. J. Dev. Biol. 57, 201-210.

Cook, M.S., Munger, S.C., Nadeau, J.H., Capel, B. (2011). Regulation of male germ cell cycle arrest and differentiation by DND1 is modulated by genetic background. Development 138, 23-32.

Dawson, E.P., Lanza, D.G., Webster, N.J., Benton, S. M., Suetake, I. and Heaney, J.D. (2018). Delayed male germ cell sex-specification permits transition into embryonal carcinoma cells with features of primed pluripotency. Development 145, dev156612. doi:10.1242/dev.156612.

Fiorenzano, A., Pascale E., D'Aniello, C., Acampora, D., Bassalert, C., Russo, F., Andolfi, G., Biffoni, M., Francescangeli, F., Zeuner, A., Angelini, C., Chazaud, C, Patriarca, E.J., Fico, A., Minchiotti, G. (2016). Cripto is essential to capture mouse epiblast stem cell and human embryonic stem cell pluripotency. Nature Commun.7, 12589.

Gu, W., Mochizuki, K., Otsuka, K., Hamada, R., Takehara, A., Matsui, Y. (2018). Dnd1-mediated epigenetic control of teratoma formation in mouse. Biol. Open 7, bio030106.

Hayashi, K., Ohta, H., Kurimoto, K., Aramaki, S., Saitou, M. (2011). Reconstitution of the mouse germ cell specification pathway in culture by pluripotent stem cells. Cell 146, 519-532.

Hackett, J.A., Surani, M.A. (2014). Reguratory principles of pluripotency: From the ground state up. Cell Stem Cell 15, 416-4130.

Hescheler, J., Fleischmann, B. K., Lentini, S., Maltsev, V. a, Rohwedel, J., Wobus, a M., Addicks, K. (1997). Embryonic stem cells: a model to study structural and functional properties in cardiomyogenesis. Cardiovasc Res 36, 149–162.

Kanatsu-Shinohara, M., Inoue, K., Lee, J., Yoshimoto, M., Ogonuki, N., Miki, H., Baba, S., Kato, T., Kazuki, Y., Toyokuni, S., Toyoshima, M., Niwa, O., Oshimura, M., Heike, T., Nakahata, T., Ishino, F., Ogura, A., Shinohara, T. (2004). Generation of pluripotent stem cells from neonatal mouse testis. (2004). Cell 19, 1001-1012.

Kedde, M., Strasser, M.J., Boldajipour, B., Oude Vrielink, J.A., Slanchev, K., le Sage, C., Nagel, R., Voorhoeve, P.M., van Duijse, J., Ørom, U.A., Lund, A.H., Perrakis, A., Raz, E., Agami, R. (2007). RNA-Binding Protein Dnd1 Inhibits MicroRNA Access to Target mRNA. Cell. 131, 1273-1286.

Kelly, G.M., Gatie, M.I. (2017). Mechanisms regulating Sstemness and differentiation in embryonal carcinoma cells. Stem Cells Int. 2017, 3684178.

Kim, M. J., Choi H. W., Jang H. J., Chung H. M., Arauzo-Bravo M. J., Schöler H. R., and Do T. J. (2013) Conversion of genomic imprinting by reprogramming and dedifferentiation. Journal of Cell Science 126, 2516-2524.

Kimura, T., Tomooka, M., Yamano, N., Murayama, K., Matoba, S., Umehara, H., Kanai, Y., Nakano, T. (2008). AKT signaling promotes derivation of embryonic germ cells from primordial germ cells. Development 135, 869–879.

Kleinsmith, L.J., Pierce, Jr. B.P. (1964). Multipotentiality of single embryonal carcinoma cells. Cancer Res. 24, 1544-1551.

Kurimoto, K., Yabuta, Y., Ohinata, Y., Ono, Y., Uno, K.D., Yamada, R.G., Ueda, H.R.,

Saitou, M. (2006). Nucleic Acids Res. 34, e42.

Leitch, H.G., Nichols, J., Humphreys, P., Mulas, C., Martello, G., Lee, C., Jones, K., Surani, M.A., Smith, A. (2013). Rebuilding pluripotency from primordial germ cells. Stem Cell Rep. 1, 66-78.

Matsui, Y., Zsebo, K.M., Hogan, B.L.M. (1992). Derivation of pluripotent embryonic stem cells from murine primordial germ cells in culture. Cell 70, 841-847.

Matsui, Y., Takehara, A., Tokitake, Y., Ikeda, M., Obara, Y., Morita-Fujimura, Y., Kimura, T., and Nakano, T. (2014). The majority of early primordial germ cells acquire pluripotency by Akt activation. Development 141, 4457-4467.

Matsui, Y., Takehara, A., Tokitake, Y., Ikeda, M., Obara, Y., Morita-Fujimura, Y., Kimura, T., Nakano, T. (2014). The majority of early primordial germ cells acquire pluripotency by Akt activation. Development 141, 4457-4467.

Mintz, B., Illmensee, K. (1975). Normal genetically mosaic mice produced from malignant teratocarcinoma cells. Proc.Natl. Acad. Sci. USA 72, 3585–9.

Murayama, H., Masaki, H., Sato, H., Hayama, T., Yamaguchi, T. and Nakauch. H. (2017). Successful Reprogramming of Epiblast Stem Cells by Blocking Nuclear Localization of b-Catenin. Stem Cell Rep. 4, 103-113.

Nichols, J., Smith, A. (2009). Naive and Primed Pluripotent States. Cell Stem Cell 4, 487–492.

Noguchi, T., Noguchi, M. (1985). A recessive mutation (ter) causing germ cell deficiency and a high incidence of congenital testicular teratomas in 129/Sv-ter mice. J. Natl. Cancer Inst. 75, 385–92.

Papaioannou, V. E., Gardner, R. L., McBurney, M. W., Babinet, C., & Evans, M. J. (1978). Participation of cultured teratocarcinoma cells in mouse embryogenesis. J.

Embryol. Exp. Morph., 44, 93–104.

Resnick, J.L., Bixler, L.S., Cheng, L., and Donovan, P.J. (1992). Long-term proliferation of mouse primordial germ cells in culture. Nature 359, 550-551

Seisenberger, S., Andrews, S., Kruger, F., Arand, J., Walter, J., Santos, F., Popp, C., Thienpont, B., Dean, W., Reik, W. (2012). The dynamics of genome-wide DNA methylation reprogramming in mouse primordial germ cells. Mol. Cell 48, 849-862.

Sekinaka, T., Hayashi, Y., Noce, T., Niwa, H., Matsui, Y. (2016). Selective de-repression of germ cell-specific genes in mouse embryonic fibroblasts in a permissive epigenetic environment. Scientific Reports 6:32932.

Stevens, L. C., Little, C. C. (1954). Spontaneous Testicular Teratomas in an Inbred Strain of Mice. Proc.Natl. Acad. Sci. USA 40(11), 1080–1087.

Stevens, L.C. (1973). A new inbred subline of mice (129-terSv) with a high incidence of spontaneous congenital testicular teratomas. J. Natl. Cancer Inst. 50, 235-242.

Stevens, L.C. (1981). Genetic influence on the development of gonadal tumors in mice with emphasis on teratomas. H.E.Kaiser (ed.), Neoplasm-Comparative Pathology of growth in animals, plants and man.

Stevens, L.C. (1983). The origin and development of testicular, ovarian, and embryo-derived teratomas. Cold Spring Harbor Conferences on cell proliferation 10, 23-36.

Suzuki, A., Saga, Y. (2008). Nanos2 suppresses meiosis and promotes male germ cell differentiation, Genes Dev. 22, 430-435.

Ueda, T., Yamada, T., Hokuto, D., Koyama, F., Kasuda, S., Kanehiro, H., Nakajima, Y. (2010). Generation of functional gut-like organ from mouse induced pluripotent stem cells. Biochem. and Biophys. Res. Commun. 391, 38–42.

Yamaguchi, S., Hong, K.,, Liu, R., Shen, L., Inoue, A., Diep, D., Zhang, K., Zhang, Y. (2012). Tet1 controls meiosis by regulating meiotic gene expression. Nature 492, 444-447.

Yamaji M., Jishage M., Meyer C., Suryawanshi H., Der E., Yamaji M., Garzia A., Morozov P., Manickavel S., McFarland H.L., Roeder R.G., Hafner M., Tuschl T. (2017) DND1 maintains germline stem cells via recruitment of the CCR4–NOT complex to target mRNAs. Nature. 543, 568-572.

Yoshimizu, T., Sugiyama, N., De Felice, M., Yeom, Y.I., Ohbo, K., Masuko, K., Obinata, M., Abe, K., Schöler, H.R., Matsui, Y. (1999). Germline-specific expression of the Oct4/green fluorescent protein (GFP) transgene in mice. Dev. Growth Differ. 41, 675-684.

Youngren, K.K., Coveney, D., Peng, X., Bhattacharya, C., Schmidt, L.S., Nickerson, M.L., Lamb, B.T., Deng, J.M., Behringer, R.R., Capel, B., Rubin, E.M., Nadeau, J.H., Matin, A. (2005). The Ter mutation in the dead end gene causes germ cell loss and testicular germ cell tumors. Nature. 435, 360-364.

Watanabe, K., Kamiya, D., Nishiyama, A., Katayama, T., Nozaki, S., Kawasaki, H., Watanabe, Y., Mizuseki, K., and Sasai, Y. (2005). Directed differentiation of telencephalic precursors from embryonic stem cells. Nature Neurosci. 8, 288-296.

Wu, J., Daiji Okamura, D., Li, M., Suzuki, K., Luo, C., Ma, L., He, Y., Li, Z., Benner, C., Tamura, I., Krause, M.N., Nery, J.R., Du, T., Zhang, Z., Hishida, T., Takahashi, Y., Aizawa, E., Kim, N.Y., Lajara, J., Guillen, P., Campistol, J.M., Esteban, C.R., Ross, P.J., Saghatelian, A., Ren, B., Ecker, J.R., Izpisua Belmonte, J.C. (2015). An alternative pluripotent state confers interspecies chimeric competency. Nature 521, 316-321.

Yoshinaga, K., Muramatsu, H., Muramatsu, T. (1991). Immunohistochemical localization of the carbohydrate antigen 4C9 in the mouse embryo a reliable marker of

mouse primordial germ cells. Differentiation. 48, 75-82.

Figure legends

Fig. 1

The appearance of teratoma-forming cells in peri- and post-natal *Dnd1*$^{ter/ter}$ testes. HE-staining (A) and immunostaining for SSEA1 (B) in the *Dnd1*$^{ter/ter}$ testis and *Dnd1*$^{ter/+}$ or *Dnd1*$^{+/+}$ testis at E18.5, P2, P4, and P7. Insets show higher magnification images of the rectangular areas. Brown staining in (B) indicates SSEA1-positive cells. Scale bars: 200 μm for main photomicrographs, and 100 μm for insets.

Fig. 2

Derivation of cell lines from teratoma-forming cells in the *Dnd1*$^{ter/ter}$ testis at P2. (A, B) Appearance of Oct4-deltaPE-GFP-positive clusters of teratoma-forming cells in the *Dnd1*$^{ter/ter}$ testis at P2. Whole-mount images of the testes and isolated cell masses containing GFP-positive cells (A), and immunostaining for 4C9, GFP expression, and DAPI staining in a section of the testis shown in A (B). (C) Primary (upper two rows) and tertiary (third row) cultures of teratoma-forming cells. The bottom row shows an established CDGC cell line, CDGC1-P3-9, after cloning. (D) CDGC1-P3-9 cultured in the 2i/LIF condition. Scale bars: 500 μm for (A), 100 μm for inset in (A), and 250 μm for (B, C, D).

Fig. 3

Quantification of pluripotent marker gene expression in CDGC1-P3-9, CDGC6-P5-6, and ESCs (E14tg2a) cultured in serum/LIF medium, and EpiSCs. Expression of the core pluripotency (A), naïve pluripotency (B), and primed pluripotency marker genes (C) was determined by quantitative RT-PCR (RT-qPCR). Data were obtained from three independent experiments. Error bars show mean ± SD**.** *$p < 0.05$, **$p < 0.01$, ***$p < 0.001$, n.s.; not significant.

Fig. 4

Transcriptomic analysis of CDGCs. (A) Scatter plot showing log10 fragments per kilobase of exon per million reads mapped (FPKM) from RNA-seq data of CDGC1-P3-

9, CDGC6-P5-6, *Dnd1*-KD ESCs (E14tg2a), and control ESCs (E14tg2a) cultured in serum/LIF medium (data were obtained from two biological replicates of RNA-seq. GSE118582; Table S1), and EpiSCs_1 (SRR3317447_1, SRR3317447_2). Red and blue dots indicate genes with log2 fold change >2 or <−2, respectively. (B) Principal component analysis of CDGC1-P3-9, CDGC6-P5-6, control E14tg2a ESCs, *Dnd1*-KD E14tg2a ESCs (this study; GSE118582), D3 GFP ESC (SRR827706, SRR827707), EpiSC_1 (SRR3317447), EpiSC_2 (SRR1660269, SRR1660270), E11.5 male(m)PGCs (SRR648693, RSS648694), E13.5 mPGCs (SRR649339, SRR649340), and E16.5 male germ cells (mGS) (ERR192339;). *x* axis: Component 1 (62.87%), *y* axis: Component 2 (11.65%), *z* axis: Component 3 (6.17%).

Fig. 5

Differentiation potential of CDGC1-P3-9. (A) Differentiation of CDGC1-P3-9 cultured in serum/LIF medium into α-smooth muscle actin (α-SMA) -positive mesodermal cells, β-tubulin-positive neural cells, and FOXA2-positive endodermal cells. Scale bars: 100 μm. (B) Male (left) and female (right) chimeric mice obtained from CDGC1-P3-9 cultured in 2i/LIF medium.

Fig. 6

The DNA methylation status of paternally imprinted *H19* and *Igf2*, and of maternally imprinted *Snrpn*, in CDGC1-P3-9 (A) and CDGC6-P5-6 (B). DNA methylation was determined by bisulfite sequencing. The filled and open circles indicate methylated and un-methylated CpGs, respectively. The data from two independent experiments were combined. The percentage of methylated CpGs is shown below each block of circles.

Fig. 7

Single-cell RT-qPCR of the teratoma-forming cells. The expression of pluripotency marker genes, and of *Arbp* as an internal control, in single teratoma-forming cells randomly selected from an Oct4-deltaPE-GFP-expressing cell cluster in the *Dnd1*$^{ter/ter}$ testis at P2 (Teratoma; yellow bars) and in single Blimp1-mVenus;Stella-ECFP (BVSC) ESCs cultured in 2i/LIF medium (ESC; blue bars) was quantitatively determined by RT-qPCR. Results for 15 teratoma-forming cells (Teratoma_#7-21) are shown. Data in (A)-(D) were obtained in distinct PCR experiments. Vertical axis indicates Ct values of RT-

qPCR.

Fig. S1

Established CDGC6-P5-6 cultured in serum/LIF (A) or 2i/LIF (B) medium. Scale bars: 250 μm.

Fig. S2

Immunostaining for OTX2 of BVSC ESCs cultured in 2i/LIF medium and EpiLCs differentiated from BVSC ESCs (A), and CDGCs cultured in serum/LIF medium (B). Right panels of each cell line show the magnified views of the boxed areas in the respective left panels. Arrowheads and arrows in (B) indicate cells with strong and weak Oct4-deltaPE-GFP signals, respectively. Scale bars: 50 μm.

Fig. S3

Quantification of pluripotent marker gene expression in CDGC1-P3-9, CDCG6-P5-6, and BVSC ESCs cultured in 2i/LIF medium. The expression of the core pluripotency (A), naïve pluripotency (B), and primed pluripotency marker genes (C) was determined by quantitative RT-PCR (RT-qPCR). Data were obtained from three independent experiments. Error bars show mean ± SD**.** p-values are indicated**.**

Fig. S4

A heat map showing expression of pluripotency genes and male germ cell marker genes in CDGC1-P3-9, CDGC6-P5-6, control E14tg2a ESCs, (data were obtained from two biological replicates of RNA-seq. GSE118582), E11.5 male(m)PGCs (SRR648693, RSS648694), E13.5 mPGCs (SRR649339, SRR649340), and E16.5 male germ cells (mGS) (ERR192339). Relative miRNA expression is described according to the color scale. Red and blue indicate high and low expression, respectively. Corresponding fragments per kilobase of exon per million reads mapped (RPKM) values of the RNA-seq data are shown in Table S2.

Fig. S5

CDGC1-P3-9 cultured in the ESC condition (serum/LIF; the first column) and in the EpiSC condition after three passages (the second column). The cells were stained with

anti-OCT4 antibody. Scale bars: 100 μm.

Fig. S6

Differentiation of CDGC6-P5-6 cultured in serum/LIF medium into α-smooth muscle actin(α-SMA) -positive mesodermal cells, β-tubulin-positive neural cells, and FOXA2-positive endodermal cells.

Fig. S7

Single-cell RT-qPCR of teratoma-forming cells. The expression of pluripotency marker genes, and of *Arbp* as an internal control, in single teratoma-forming cells randomly selected from an Oct4-deltaPE-GFP-expressing cell cluster in the *Dnd1*$^{ter/ter}$ testis at P2 (Teratoma; yellow bars) and in single BVSC ESCs cultured in 2i/LIF medium (ESC; blue bars) was quantitatively determined by RT-qPCR. Results for six teratoma-forming cells (Teratoma_#1-6) are shown. Data in (A)-(E) were obtained in distinct PCR experiments. The vertical axis indicates Ct values of RT-qPCR.

Table S1

List of genes exhibiting significant ($q < 0.05$) up-regulation or down-regulation (log2 fold change >2 or <−2, respectively) between ESCs (E14tg2a) and CDGC1-P3-9, between ESCs and CDCG6-P5-6, between EpiSCs and CDGC1-P3-9, and between ESCs and *Dnd1*-KD ESCs.

Table S2

RPKM values of pluripotency and male germ cell marker genes. The data presented here correspond to those used in Fig. S4.

Table S3

PCR primers used in this study.

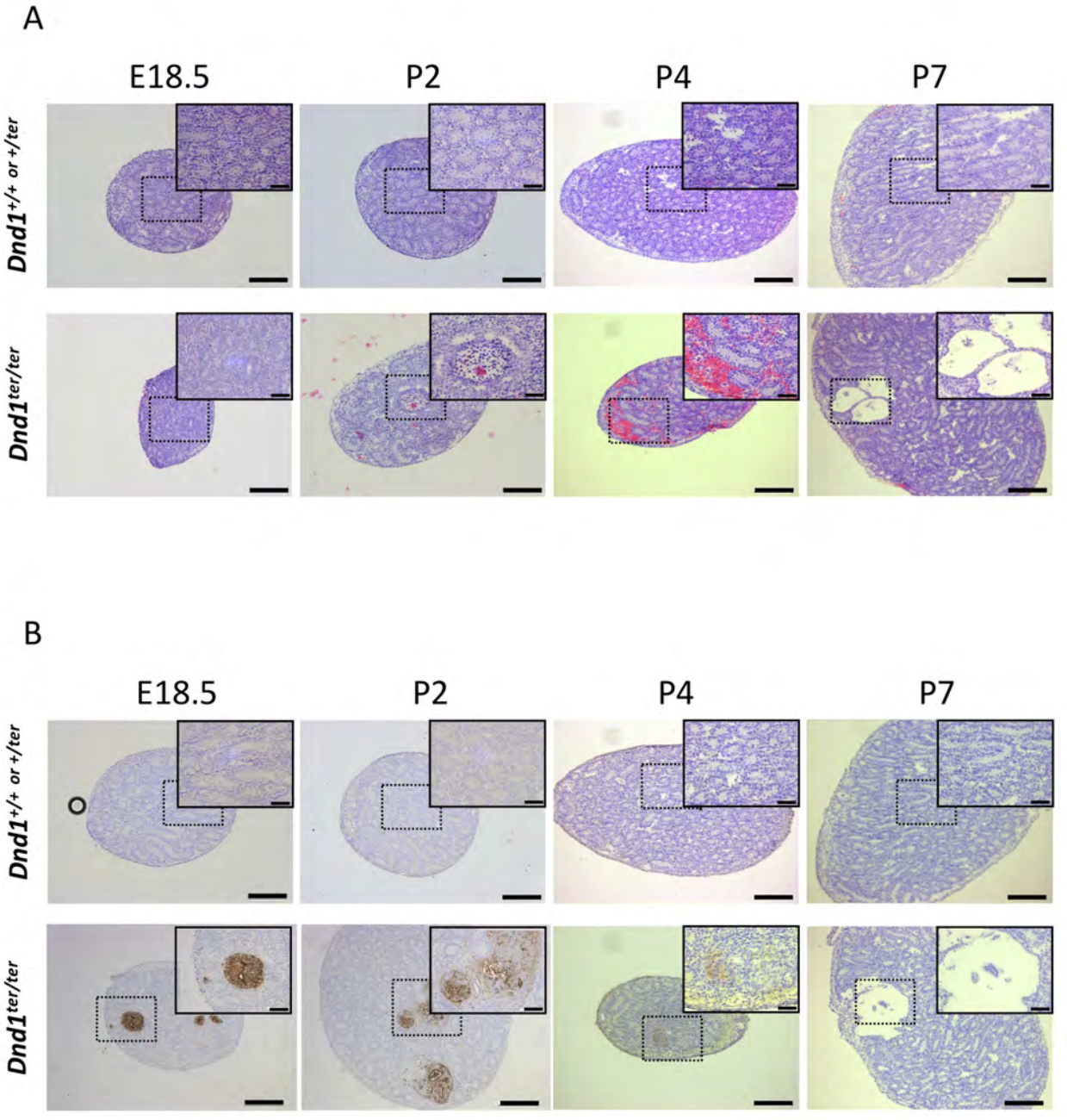
A
E18.5
P2
P4
P7
Dnd1+/+ or +/ter
Dnd1ter/ter
B
E18.5
P2
P4
P7
Dnd1+/+ or +/ter
Dnd1ter/ter

Fig.1

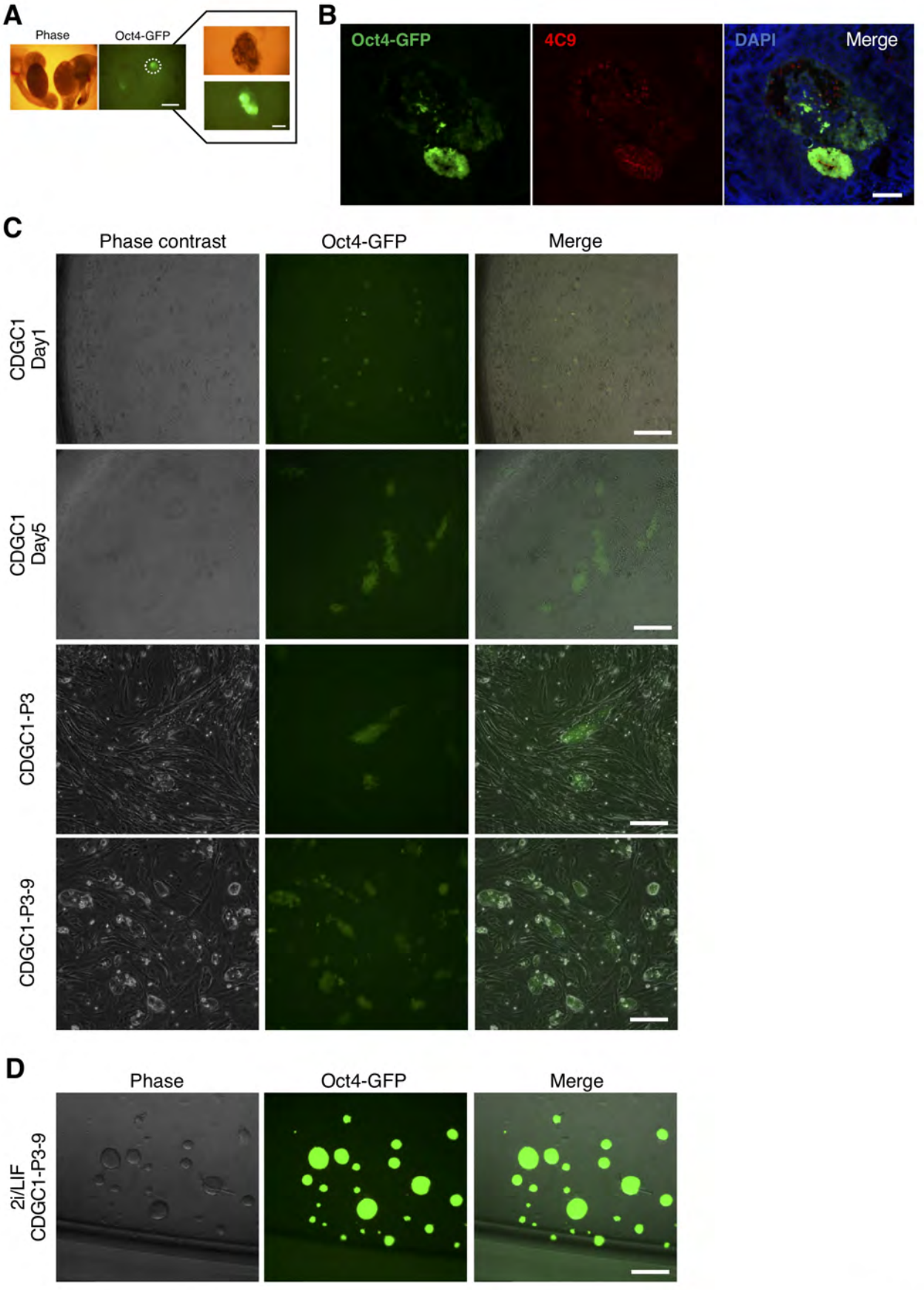
A
Phase
Oct4-GFP
B
Oct4-GFP
4C9
DAPI
Merge
C
Phase contrast
Oct4-GFP
Merge
CDGC1 Day1
CDGC1 Day5
CDGC1-P3
CDGC1-P3-9
D
Phase
Oct4-GFP
Merge
2i/LIF CDGC1-P3-9

Fig.2

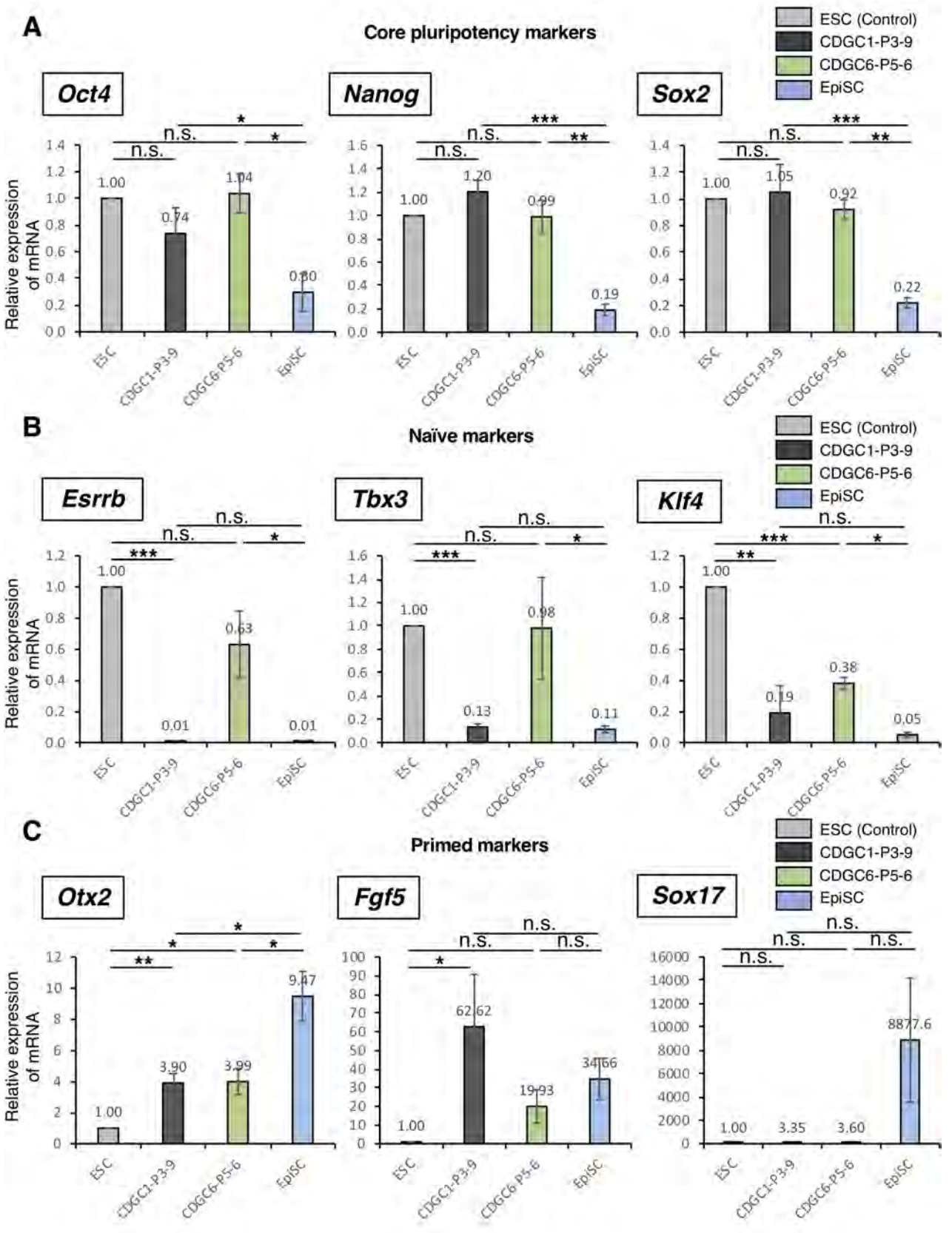
A
Core pluripotency markers
ESC (Control)
CDGC1-P3-9
CDGC6-P5-6
EpiSC
Oct4
Nanog
Sox2
Relative expression of mRNA
1.00
0.74
1.04
0.30
1.00
1.20
0.99
0.19
1.00
1.05
0.92
0.22
n.s.
*
**
***
ESC
CDGC1-P3-9
CDGC6-P5-6
EpiSC
B
Naïve markers
Esrrb
Tbx3
Klf4
1.00
0.01
0.63
0.01
1.00
0.13
0.98
0.11
1.00
0.19
0.38
0.05
C
Primed markers
Otx2
Fgf5
Sox17
1.00
3.90
3.99
9.47
1.00
62.62
19.93
34.66
1.00
3.35
3.60
8877.6

Fig.3

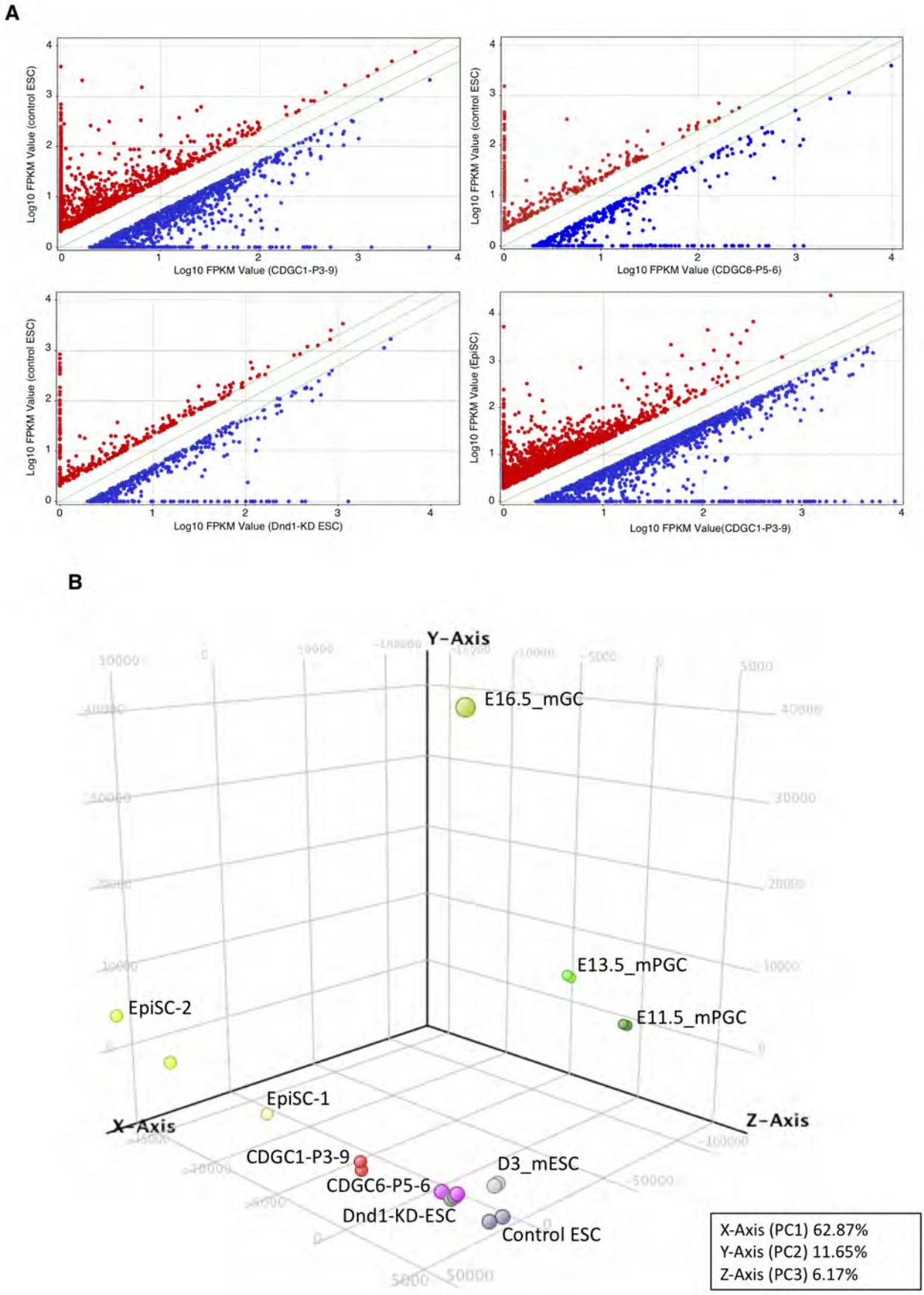
A
Log10 FPKM Value (control ESC)
Log10 FPKM Value (CDGC1-P3-9)
Log10 FPKM Value (CDGC6-P5-6)
Log10 FPKM Value (Dnd1-KD ESC)
Log10 FPKM Value (EpiSC)
Log10 FPKM Value(CDGC1-P3-9)
B
Y-Axis
X-Axis
Z-Axis
E16.5_mGC
E13.5_mPGC
E11.5_mPGC
EpiSC-2
EpiSC-1
CDGC1-P3-9
CDGC6-P5-6
Dnd1-KD-ESC
D3_mESC
Control ESC
X-Axis (PC1) 62.87%
Y-Axis (PC2) 11.65%
Z-Axis (PC3) 6.17%

Fig.4

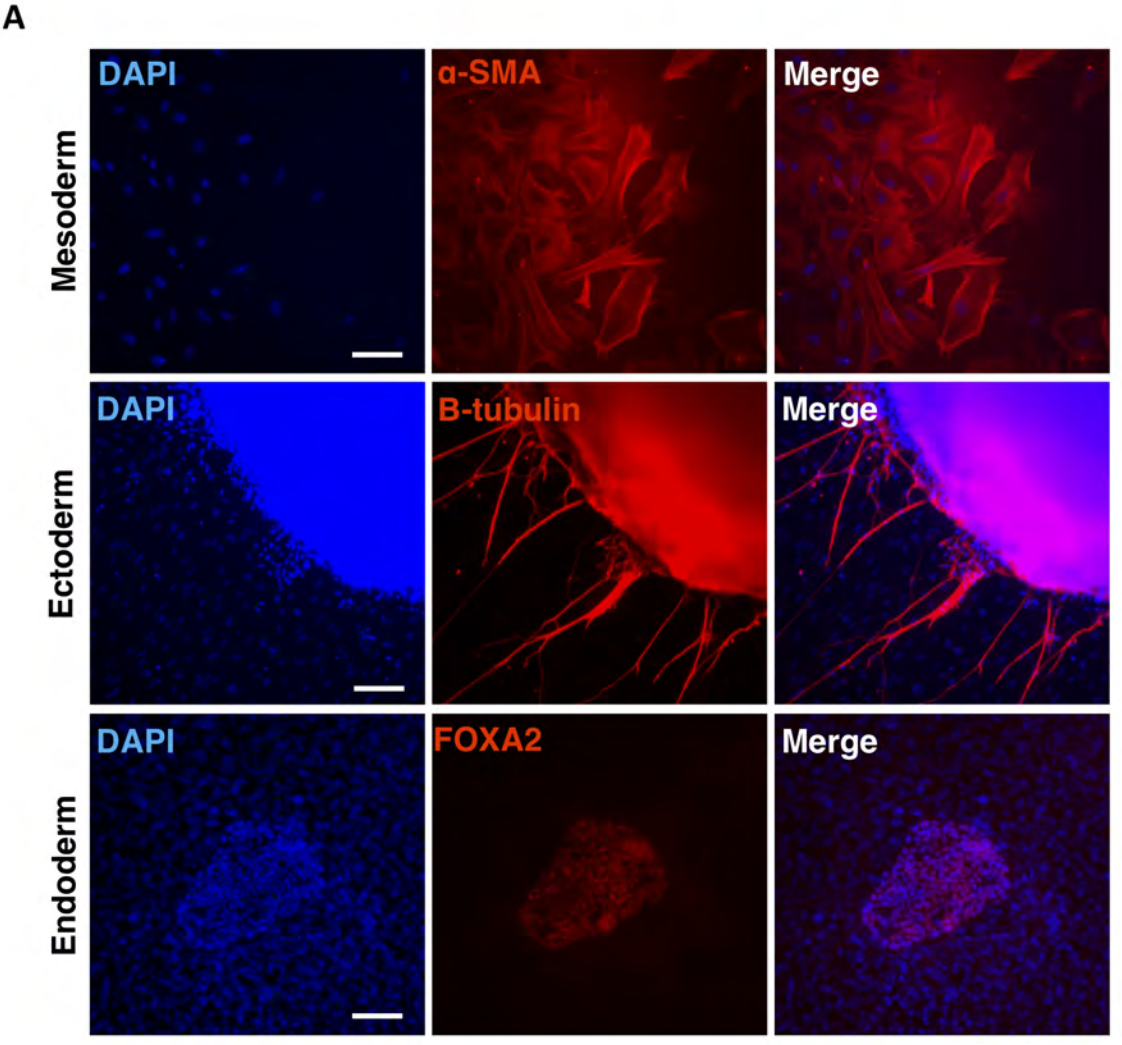
A
Mesoderm
DAPI
α-SMA
Merge
Ectoderm
DAPI
B-tubulin
Merge
Endoderm
DAPI
FOXA2
Merge
B

Fig.5

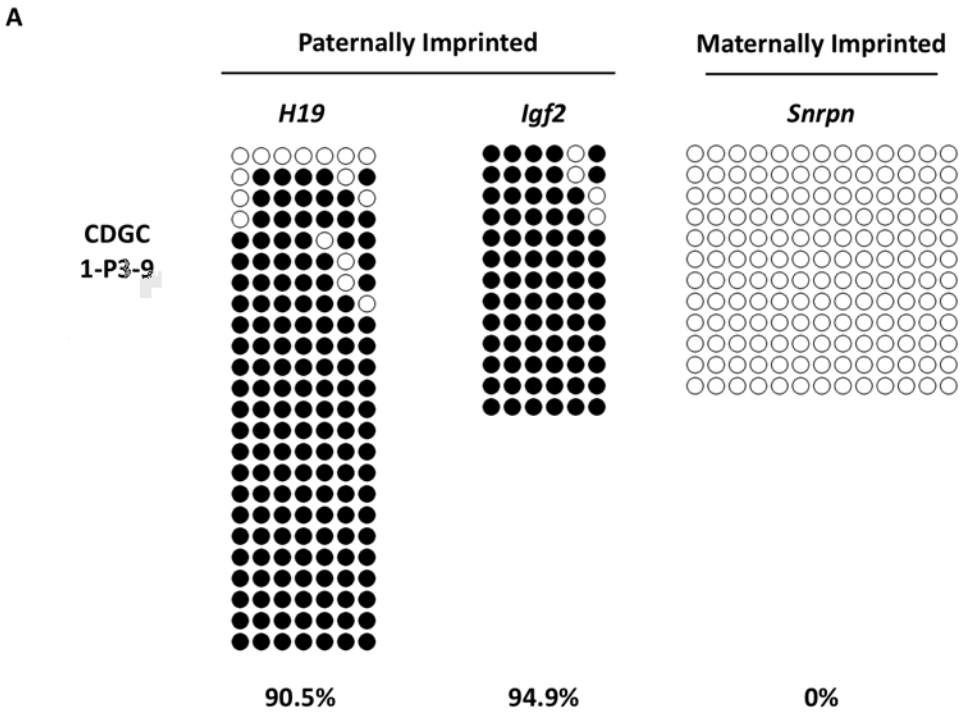
A
Paternally Imprinted
Maternally Imprinted
H19
Igf2
Snrpn
CDGC
1-P3-9
90.5%
94.9%
0%

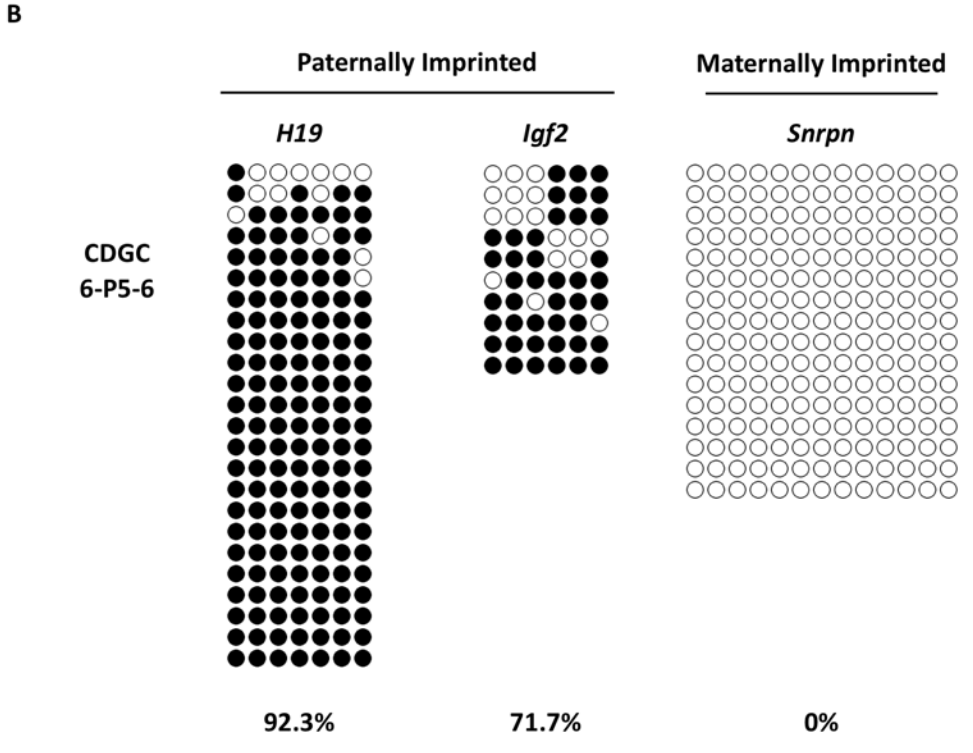
B
Paternally Imprinted
Maternally Imprinted
H19
Igf2
Snrpn
CDGC
6-P5-6
92.3%
71.7%
0%

Fig.6

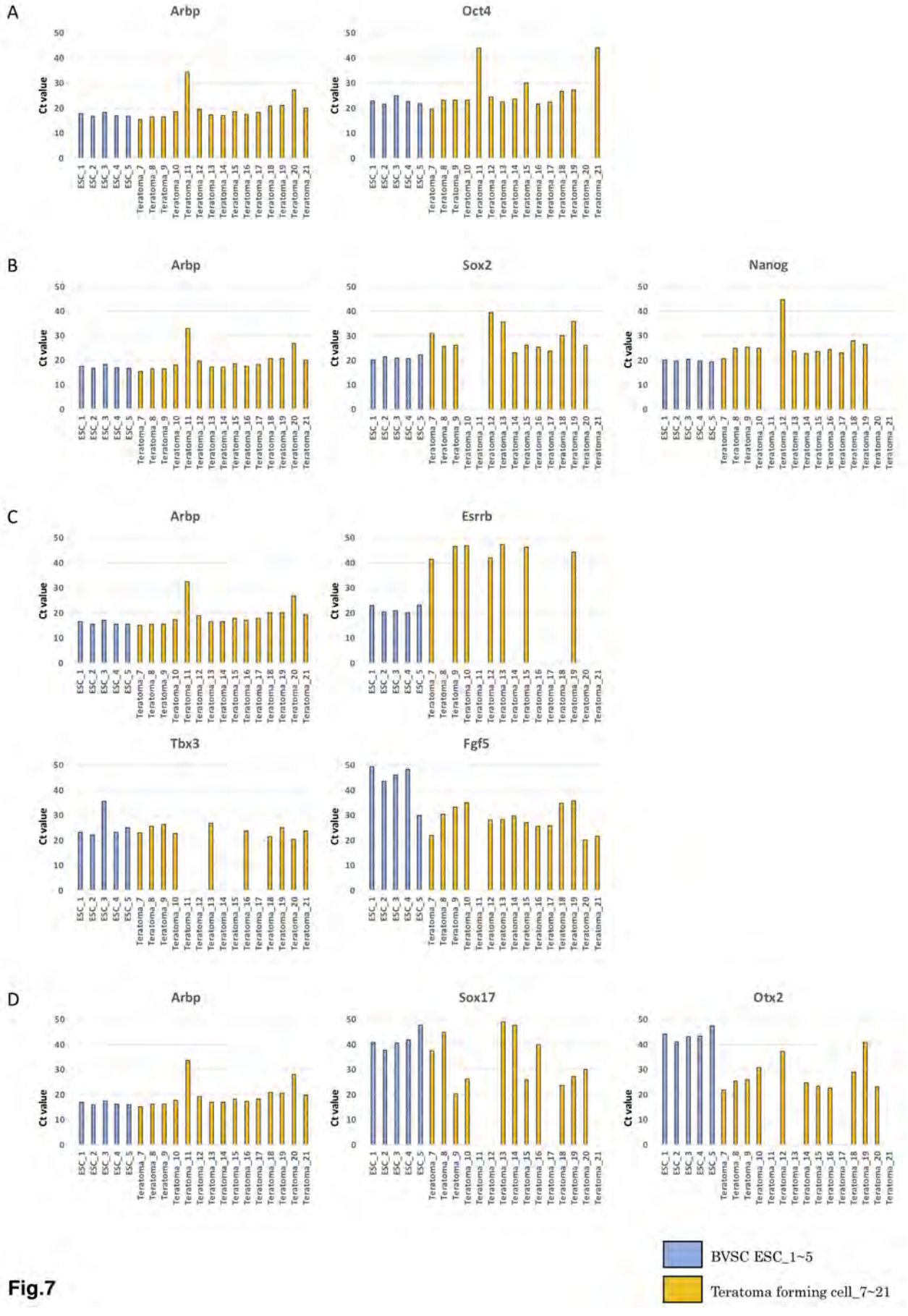
A
Arbp
Oct4
B
Arbp
Sox2
Nanog
C
Arbp
Esrrb
Tbx3
Fgf5
D
Arbp
Sox17
Otx2
Ct value
ESC_1
ESC_2
ESC_3
ESC_4
ESC_5
Teratoma_7
Teratoma_8
Teratoma_9
Teratoma_10
Teratoma_11
Teratoma_12
Teratoma_13
Teratoma_14
Teratoma_15
Teratoma_16
Teratoma_17
Teratoma_18
Teratoma_19
Teratoma_20
Teratoma_21
BVSC ESC_1~5
Teratoma forming cell_7~21

Fig.7

A

CDGC6-P5-6 (serum/LIF)

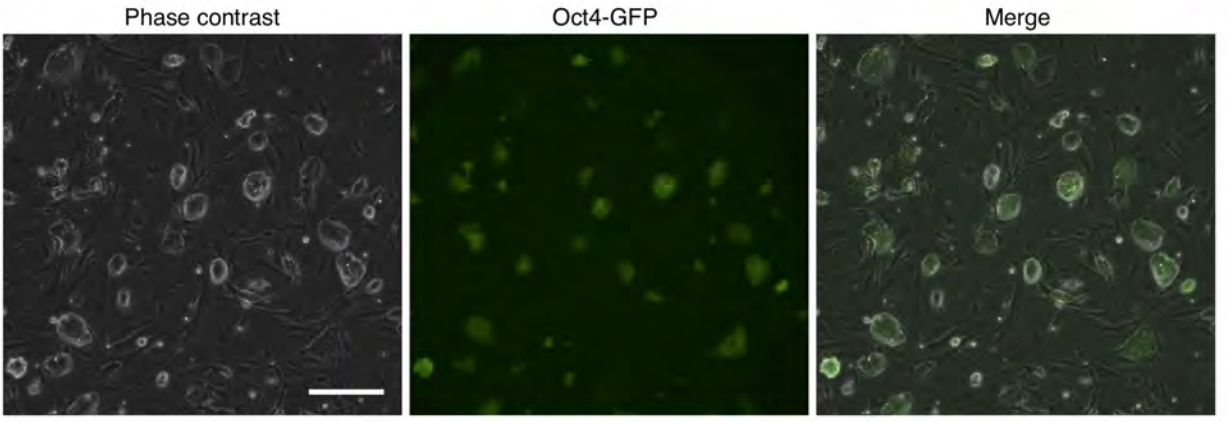

B

CDGC6-P5-6 (2i/LIF)

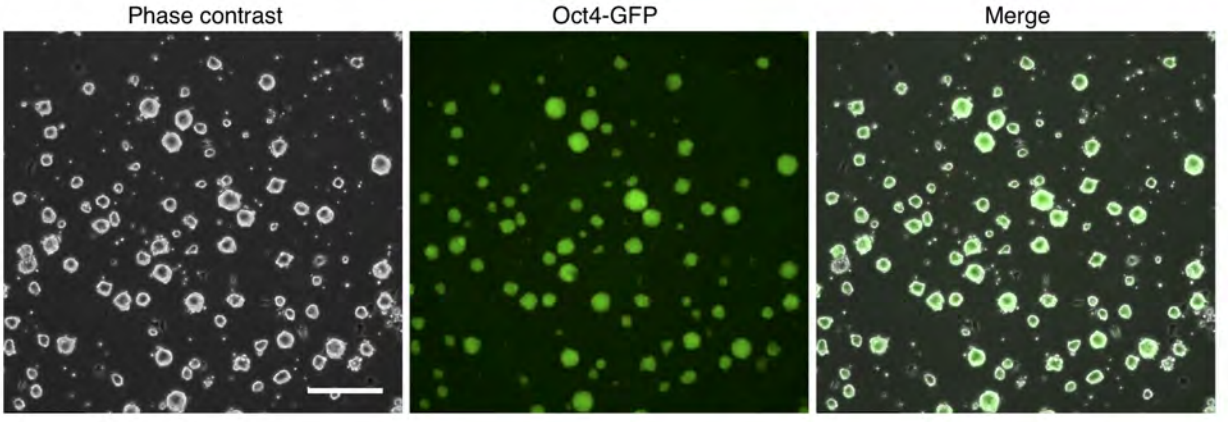

Fig.S1

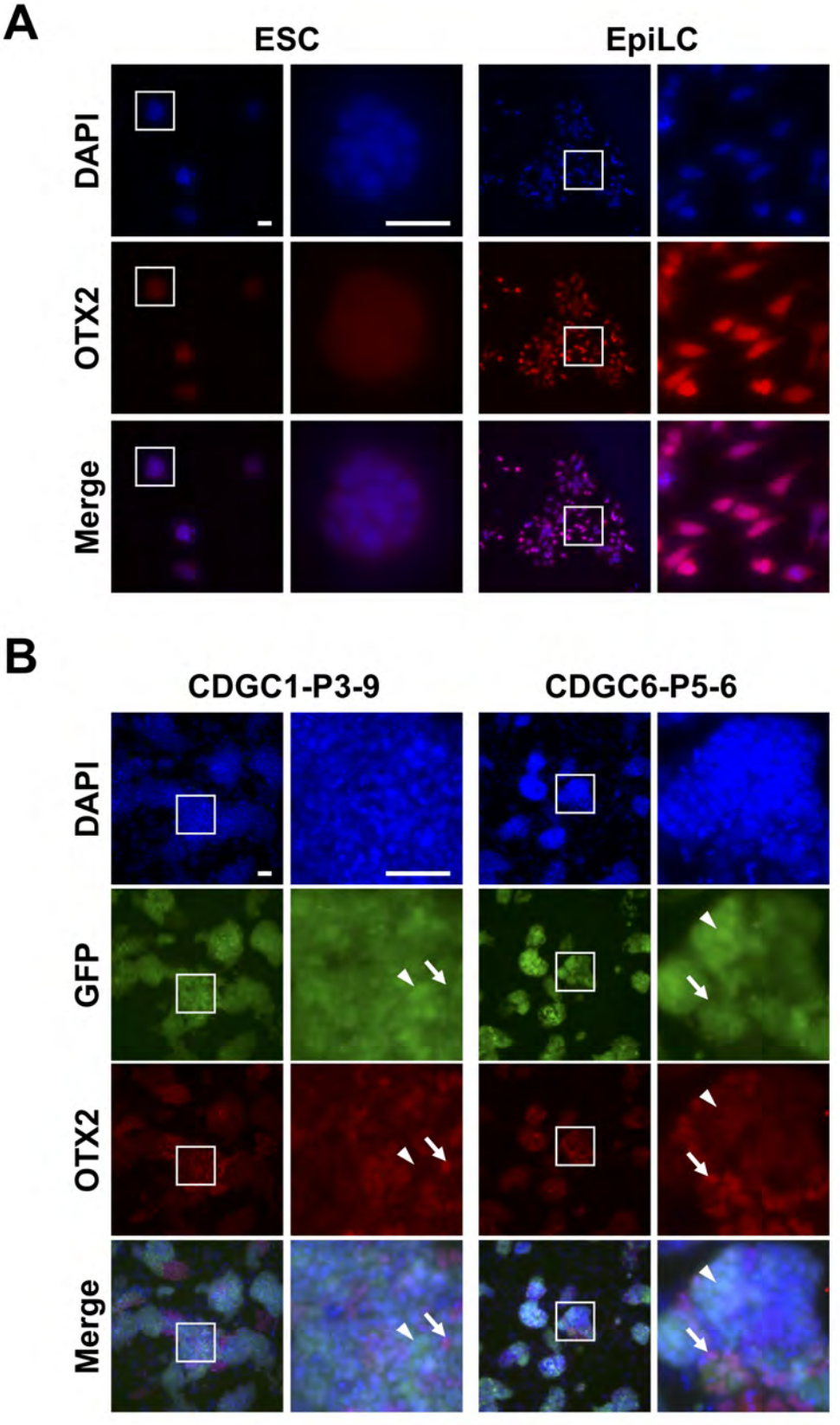
A
ESC
EpiLC
DAPI
OTX2
Merge
B
CDGC1-P3-9
CDGC6-P5-6
DAPI
GFP
OTX2
Merge

Fig.S2

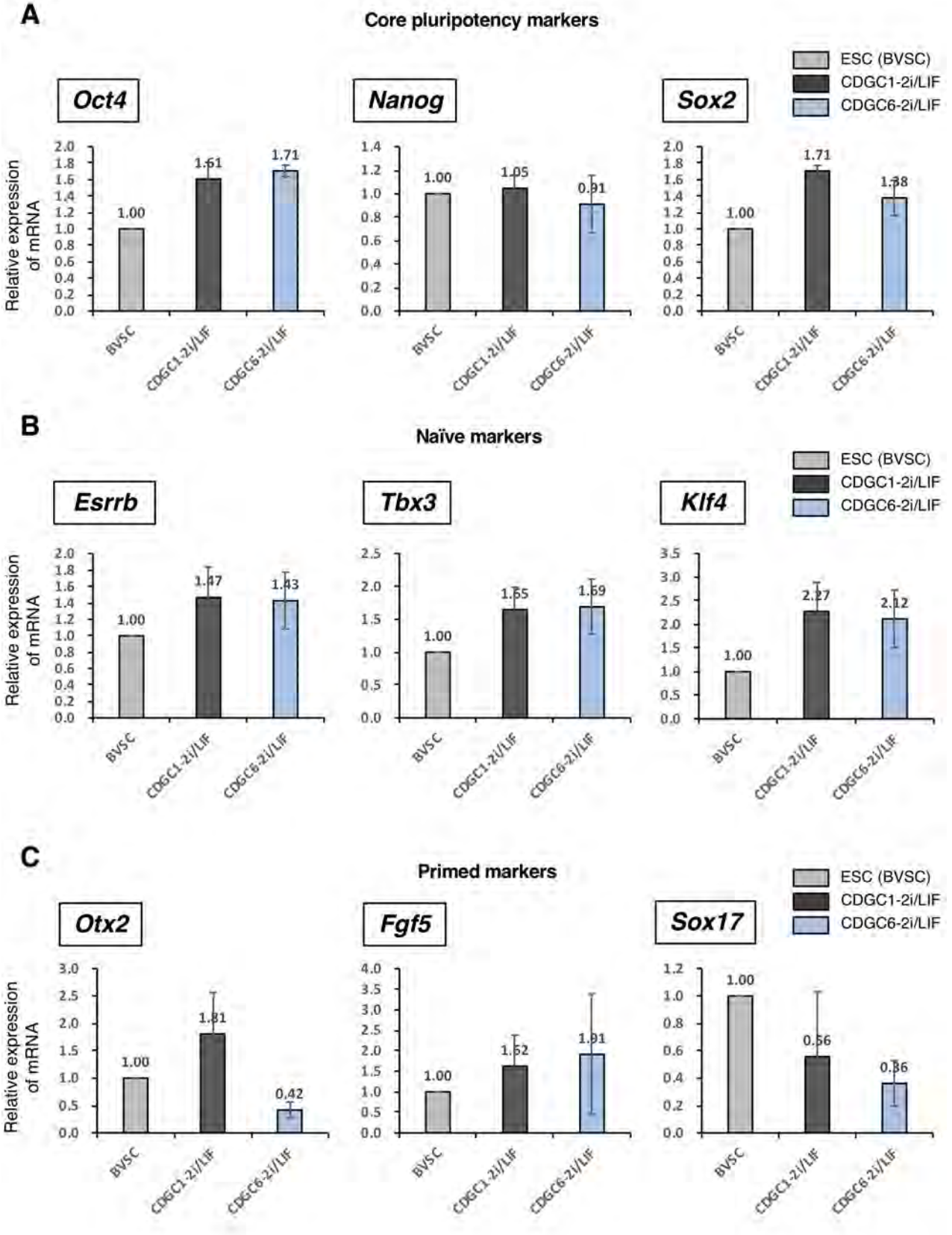
A
Core pluripotency markers
ESC (BVSC)
CDGC1-2i/LIF
CDGC6-2i/LIF
Oct4
Nanog
Sox2
Relative expression of mRNA
1.00
1.61
1.71
1.00
1.05
0.91
1.00
1.71
1.38
BVSC
CDGC1-2i/LIF
CDGC6-2i/LIF
B
Naïve markers
Esrrb
Tbx3
Klf4
1.00
1.47
1.43
1.00
1.65
1.69
1.00
2.27
2.12
C
Primed markers
Otx2
Fgf5
Sox17
1.00
1.81
0.42
1.00
1.62
1.91
1.00
0.56
0.36

Fig.S3

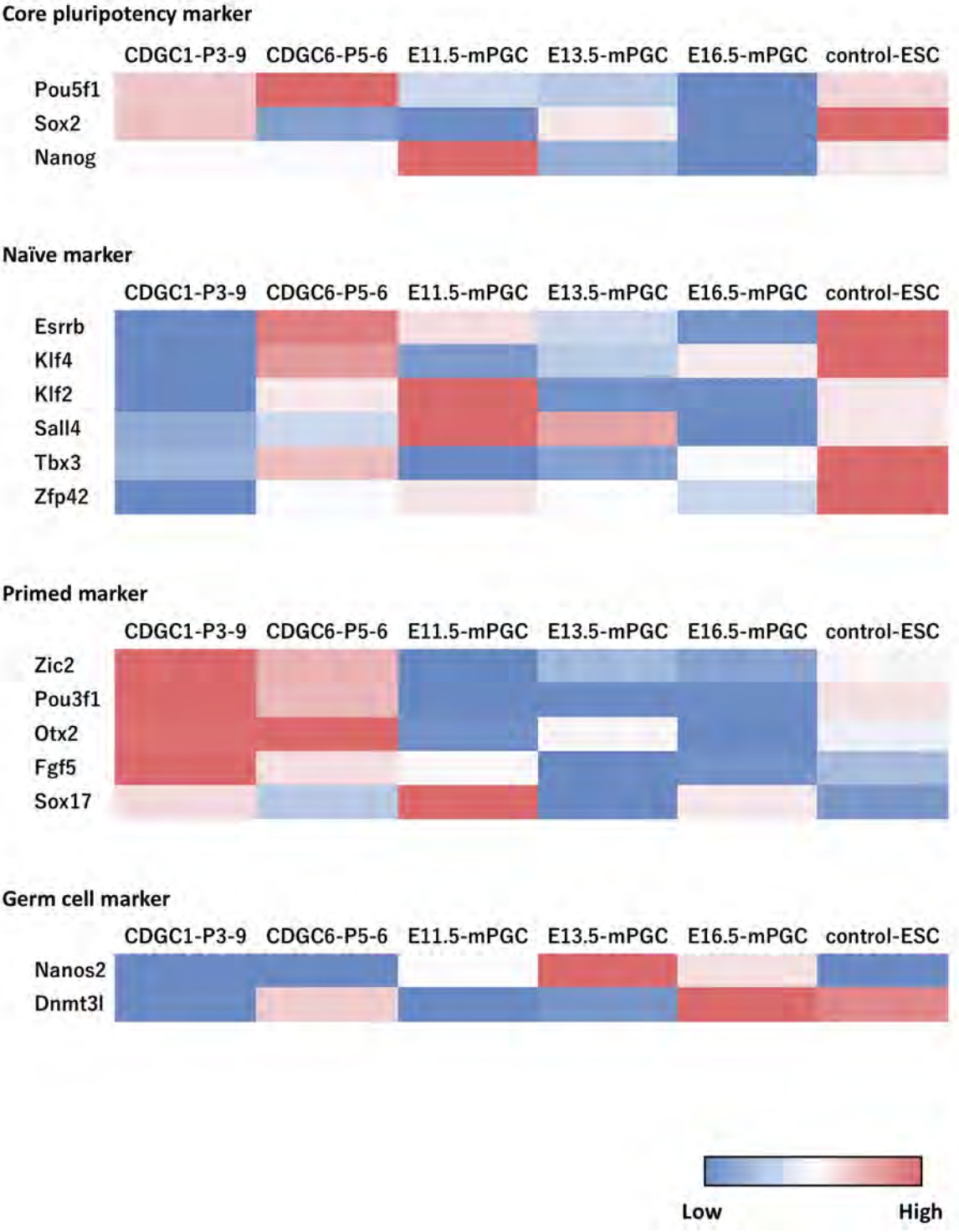
Core pluripotency marker
CDGC1-P3-9
CDGC6-P5-6
E11.5-mPGC
E13.5-mPGC
E16.5-mPGC
control-ESC
Pou5f1
Sox2
Nanog
Naïve marker
CDGC1-P3-9
CDGC6-P5-6
E11.5-mPGC
E13.5-mPGC
E16.5-mPGC
control-ESC
Esrrb
Klf4
Klf2
Sall4
Tbx3
Zfp42
Primed marker
CDGC1-P3-9
CDGC6-P5-6
E11.5-mPGC
E13.5-mPGC
E16.5-mPGC
control-ESC
Zic2
Pou3f1
Otx2
Fgf5
Sox17
Germ cell marker
CDGC1-P3-9
CDGC6-P5-6
E11.5-mPGC
E13.5-mPGC
E16.5-mPGC
control-ESC
Nanos2
Dnmt3l
Low
High

Fig.S4

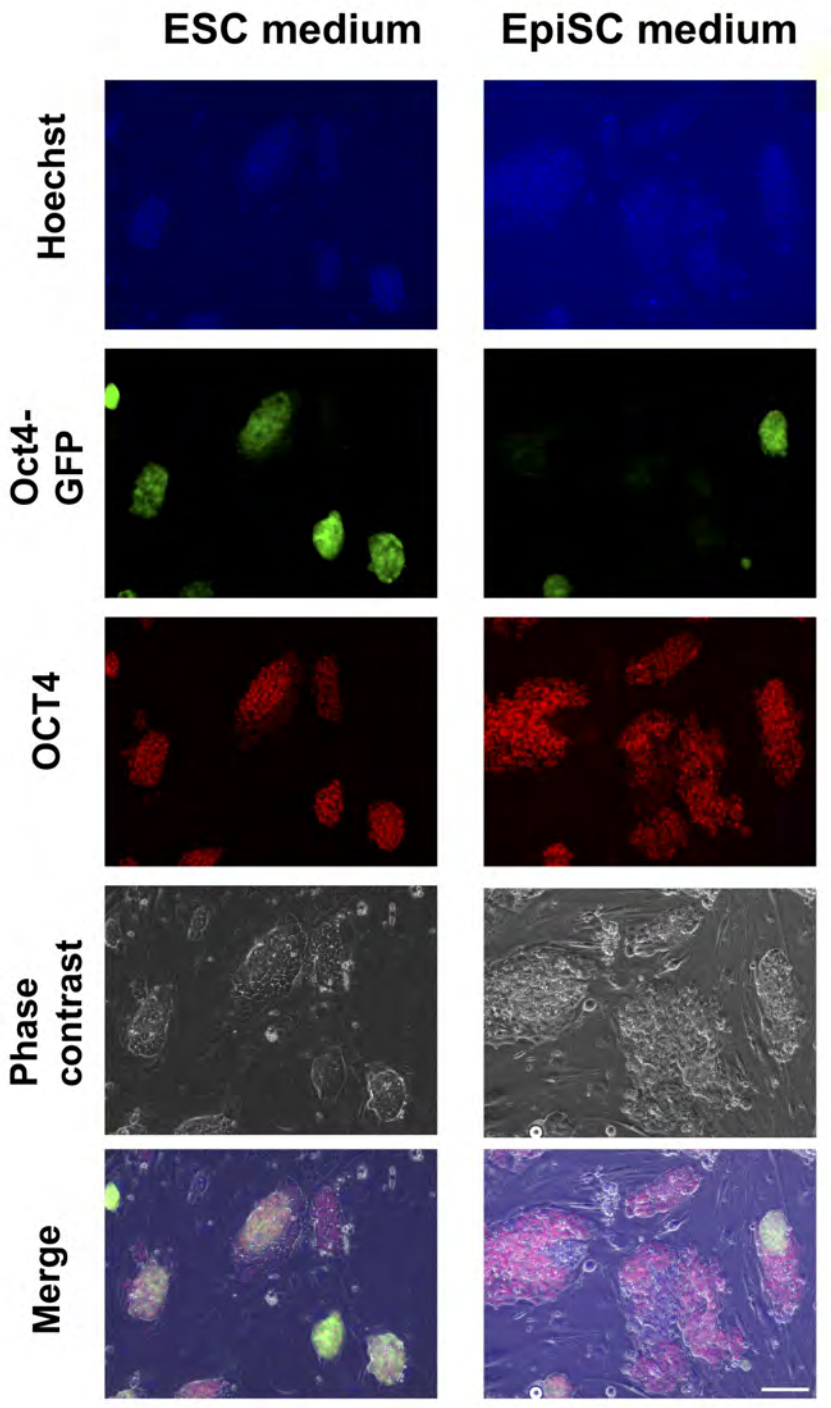
ESC medium
EpiSC medium
Hoechst
Oct4-GFP
OCT4
Phase contrast
Merge

Fig.S5

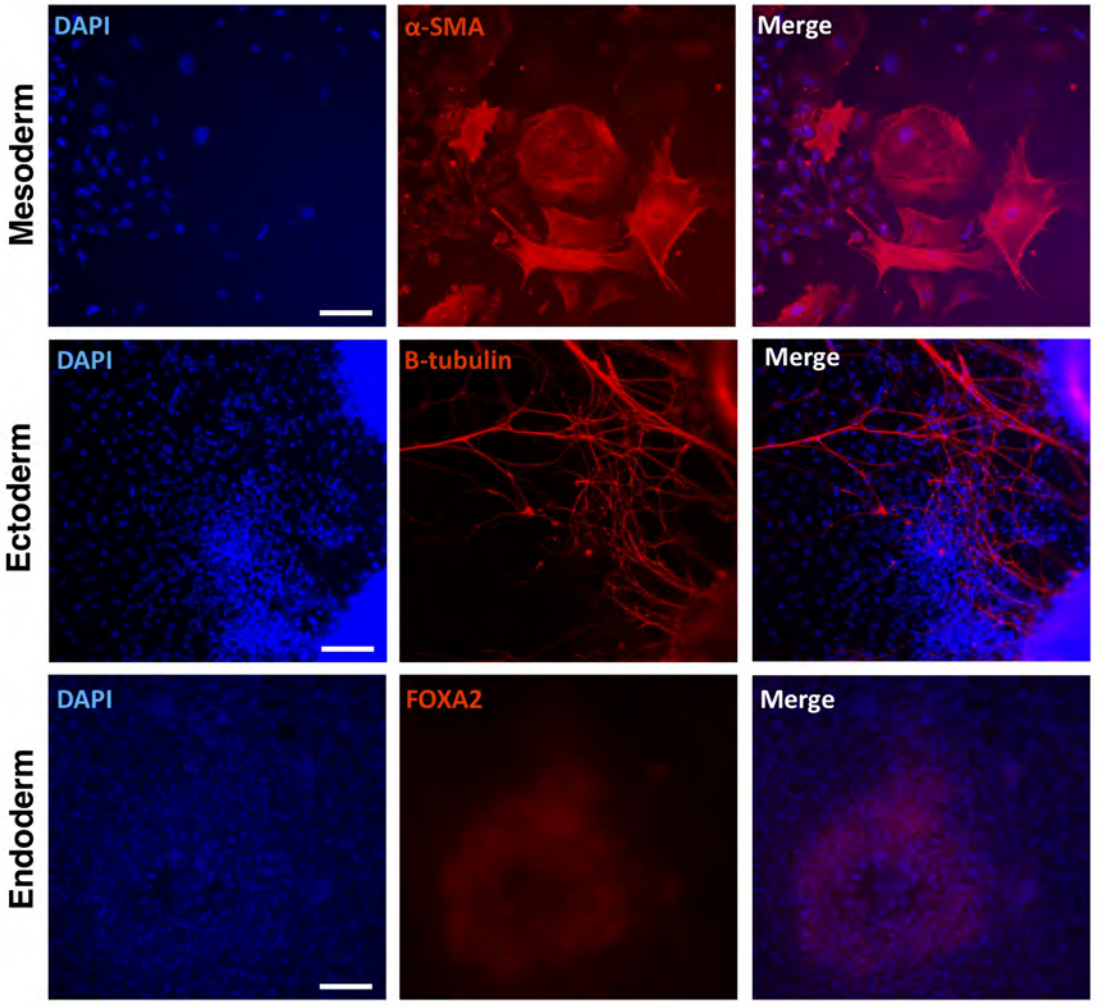
Mesoderm
DAPI
α-SMA
Merge
Ectoderm
DAPI
B-tubulin
Merge
Endoderm
DAPI
FOXA2
Merge

Fig.S6

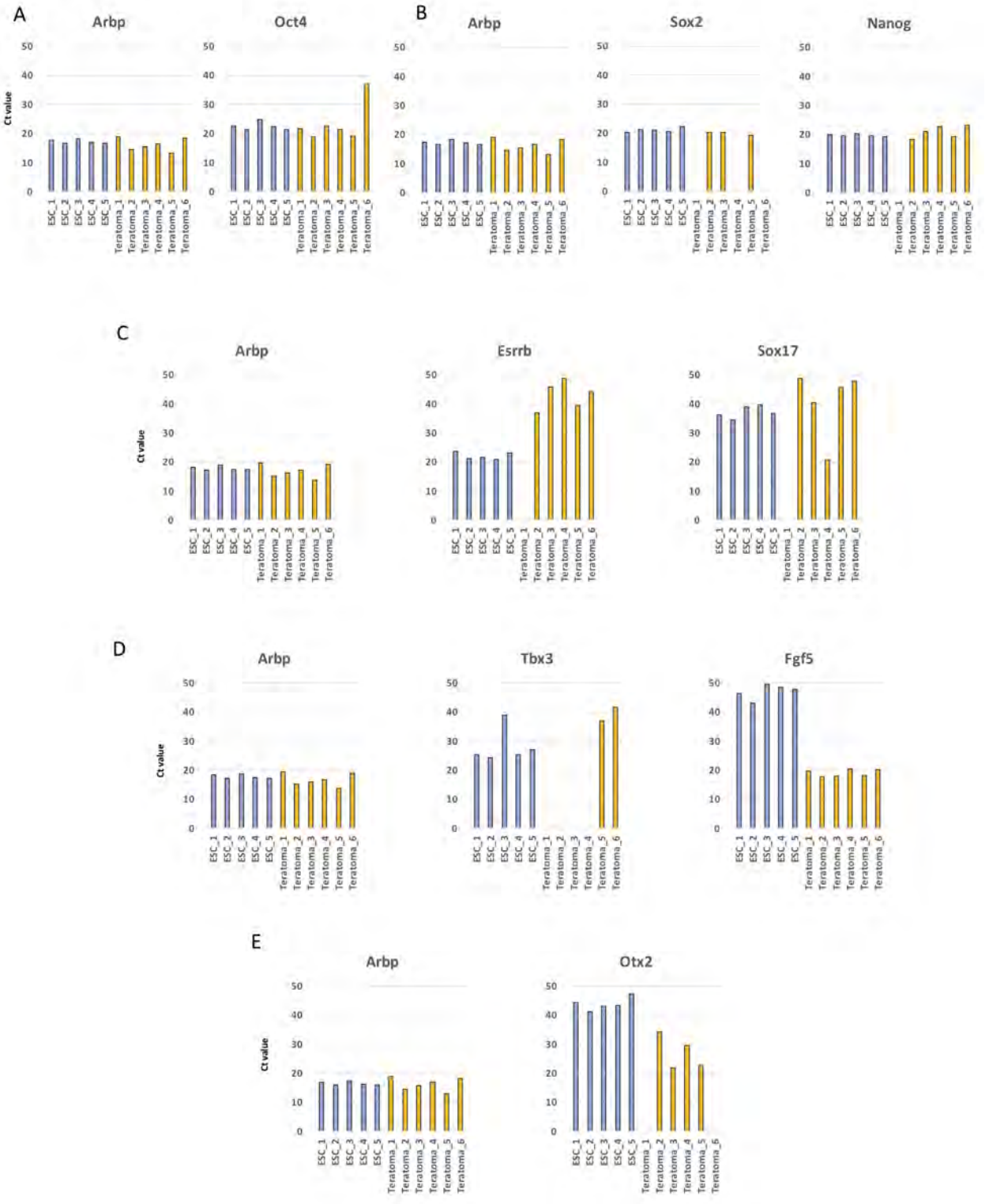
A
Arbp
Oct4
Ct value
B
Arbp
Sox2
Nanog
C
Arbp
Esrrb
Sox17
D
Arbp
Tbx3
Fgf5
E
Arbp
Otx2
ESC_1
ESC_2
ESC_3
ESC_4
ESC_5
Teratoma_1
Teratoma_2
Teratoma_3
Teratoma_4
Teratoma_5
Teratoma_6

Fig.S7